

Electronic Supplementary Information for

Crystallization Induced Emission Enhancement of Highly Electron-Deficient Dicyanomethylene-Bridged Triarylboranes

Guanming Liao^{a,b}, Jia Zhang^a, Xiaoyan Zheng^{a,*}, Xiaodi Jia^c, Jialiang Xu^c, Fenggui Zhao^a, Nan Wang^a,
Kanglei Liu^a, Pangkuan Chen^{a,*}, and Xiaodong Yin^{a,*}

^a Key Laboratory of Cluster Science, Ministry of Education of China, Beijing Key Laboratory of Photoelectronic/Electrophotonic Conversion Materials, School of Chemistry and Chemical Engineering, Beijing Institute of Technology, Beijing, 102488, P. R. China. Email: yinxdl8@bit.edu.cn, pangkuan@bit.edu.cn, xiaoyanzheng@bit.edu.cn

^b School of Chemistry and Chemical Engineering, Jiangxi Science and Technology Normal University, Nanchang, Jiangxi, 330013, P. R. China.

^c School of Materials Science and Engineering, National Institute for Advanced Materials, Nankai University, Tongyan Road 38, Tianjin, 300350 P. R. China.

Content

| | |
|--|-----|
| 1. Materials and general methods | S2 |
| 2. Experimental section | S2 |
| 3. X-ray crystallographic analyses | S7 |
| 4. Photophysical and electrochemical properties | S12 |
| 5. Theoretical calculations | S14 |
| 6. ¹H, ¹³C and ¹¹B NMR spectra | S18 |
| 7. Reference | S28 |

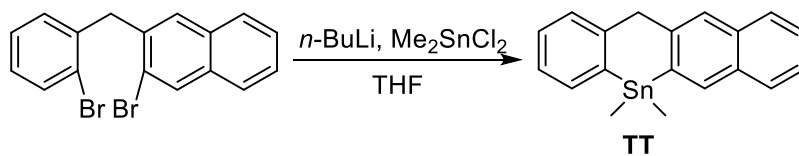
1. Materials and general methods

THF, ether and toluene were freshly distilled over sodium/benzophenone, and stored under nitrogen prior to use. Dichloromethane was distilled from CaH₂ and degassed via several freeze-pump-thaw cycles before use. All chemicals from commercial sources were used as received unless otherwise stated. Chromium(VI) oxide (CrO₃) (99.5%), malononitrile (98%), acetic acid (99.5%) and pyridine (99.5%) were purchased from Energy Chemical. BCl₃ (1 M in dichloromethane), 1,3,5-tris(trifluoromethyl)benzene (97.5%) and titanium tetrachloride (TiCl₄) (1.0 M in dichloromethane) were purchased from J&K Chemical. C₁₈ reverse silica gel chromatographic packing were purchased from Shandong Bona Biological Technology CO., Ltd.

¹H NMR (400 MHz), ¹³C NMR (101 MHz, 176 MHz) and ¹¹B NMR (128 MHz, 225 MHz) spectra were recorded on Bruker Avance 400 MHz and 700 MHz spectrometer, respectively. ¹H NMR chemical shifts were referenced to residual CHCl₃ (7.26 ppm), CH₂Cl₂ (5.32 ppm) and acetone (2.05 ppm). ¹³C NMR (proton decoupled) chemical shifts were referenced to CDCl₃ (77.16 ppm), CD₂Cl₂ (53.84 ppm), acetone-*d*₆ (29.84, 206.26 ppm). For ¹¹B NMR spectra, boron-free quartz NMR tubes were used and the spectra were referenced to external BF₃·Et₂O (δ = 0). High resolution mass spectral data were obtained on an Agilent (Q-TOF 6520) mass spectrometer. UV-Vis absorption spectra were recorded on a JASCO V-770 UV-Vis-NIR spectrophotometer. Photo-luminescent spectra were obtained on an Edinburgh Instruments FLS980 or Lengguang Tech F97PrO spectrophotometer. Fluorescent absolute quantum efficiencies were determined with a Hamamatsu C11347-11 Quantaaurus-QY spectrometer. All the photo-physical experiments of solutions are conducted using Starna quartz (3Q10) spectrophotometer cell. X-ray single crystal were recorded on a Bruker D8 X-ray single crystal Venture diffractometer. SAINT5.0 and SADABS programs are used for the reduction and absorption correction of crystal data. X-ray powder diffractions were recorded on a Bruker D8 Advance powder diffractometer. Cyclic voltammetry (CV) was measured at room temperature with glassy carbon electrode as working electrode, Platinum wire as counter electrode and Silver wire as quasi-reference electrode in deaerated DCM or THF. Ferrocene was used as the internal standard and tetrabutyl ammonium hexafluorophosphate (0.1 M) as the supporting electrolyte. The cyclic voltammograms were obtained at scan rate of 0.1 V s⁻¹ on an AUTOLAB-CV-75W voltammetric analyzer.

2. Experimental section

Synthesis of 5,5-dimethyl-5,12-dihydrobenzo[*b*]naphtho[2,3-*e*]stannine (TT)

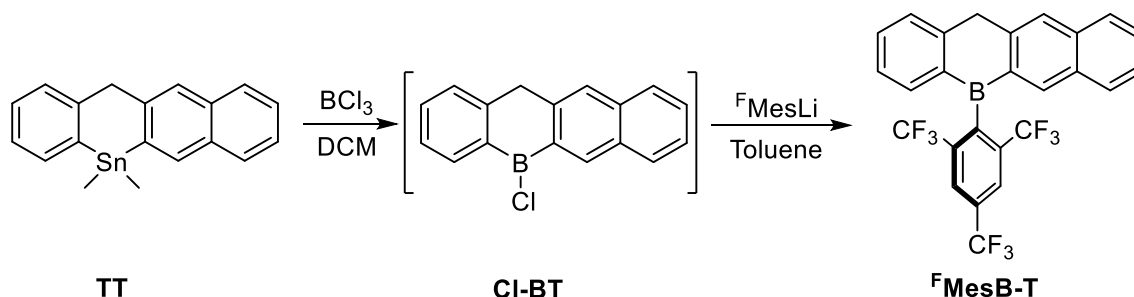


To a stirring solution of 2-bromo-3-(2-bromobenzyl)naphthalene (1.5 g, 3.98 mmol) in THF at -78°C was added *n*-BuLi (1.6 M; 5.3 mL, 8.4 mmol) dropwise and the reaction mixture was stirred for 1.5 h at the same temperature. Then, Me₂SnCl₂ (0.97 g, 4.4 mmol) in THF (2 mL) was added dropwise at -78°C. After complete addition, the mixture was allowed to cool to room temperature overnight. A saturated aqueous solution of NH₄Cl (30 mL) was added to the colorless suspension, and the mixture was stirred for 15 min. The aqueous layer was separated and extracted with Et₂O

(3 × 20 mL). The combined organic layers were washed with brine, dried with Na₂SO₄ and concentrated *in vacuo* to give a viscous yellow oil. A colorless oil was obtained by reversed-phase column chromatography, which solidified as a white solid (1.0 g, 70%) upon storage at 0°C.

¹H NMR (400 MHz, CDCl₃) δ 8.04 (s, 1H), 7.80 (s, 1H), 7.79-7.76 (m, 2H), 7.58 (dd, *J*₁ = 8.0 Hz, *J*₂ = 4.0 Hz, 1H), 7.45-7.40 (m, 3H), 7.30-7.20 (m, 2H), 4.15 (s, 2H), 0.62 (s, 6H). ¹³C NMR (101 MHz, CDCl₃) δ 147.16, 143.29, 141.02, 139.65, 136.35, 136.05, 133.96, 132.02, 129.02, 128.37, 127.62, 127.34, 126.20, 126.10, 125.64, 125.51, 46.84, -9.94. HR-ESIMS (*m/z*): [*M* + *H*]⁺ calcd. for C₁₉H₁₉Sn, 367.0530; found: 367.0499.

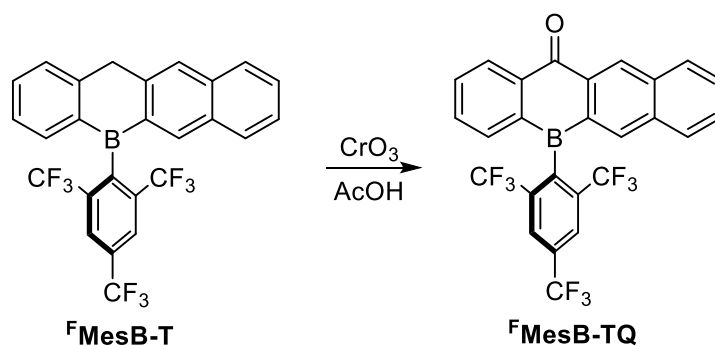
Synthesis of 5-(2,4,6-tris(trifluoromethyl)phenyl)-5,12-dihydrobenzo[*b*]naphtho[2,3-*e*]borinine (^FMesB-T)



To a stirring solution of **TT** (1.0 g, 2.74 mmol) in dichloromethane at -78°C was added BCl₃ (1 M; 4.11 mL, 4.11 mmol) dropwise. The reaction mixture was allowed to slowly come to room temperature. The volatile compounds were removed under dynamic vacuum. The resultant off white solid was transferred to a sublimation vessel and the residual Me₂SnCl₂ was removed at ambient temperature under dynamic vacuum, leaving a grey solid **Cl-BT** (0.61 g, 85%). The product is extremely sensitive toward oxygen and water that should be handled accordingly. 1,3,5-Tris(trifluoromethyl)benzene (0.98 g, 3.48 mmol) was charged into a flame-dried Schlenk flask under nitrogen atmosphere and 35 mL of dry ether were added. The flask was cooled to -78 °C and was added *n*-BuLi (1.6 M; 2.4 mL, 3.83 mmol) dropwise. The mixture was stirred for 0.5 h at -78 °C, then warmed to room temperature and stirred for 4 h. The solvent was removed under high vacuum to obtain the ^FMesLi as light yellow solid. The ^FMesLi was redissolved in 15 mL of dry toluene and the mixture was cooled to -78 °C. A solution of **Cl-BT** (0.61 g, 2.32 mmol) in 15 mL dry toluene was added to the above solution, then the mixture was allowed to warm to room temperature and stirred overnight. The reaction was quenched by adding 20 mL of water. The aqueous layer was separated and extracted with dichloromethane (3 × 10 mL). The combined organic layers were washed with brine (30 mL), dried with Na₂SO₄ and the solvent was removed *in vacuo*. The crude product was purified by column chromatography on silica gel using petroleum ether as an eluent to give **^FMesB-T** as a yellow solid (0.53 g, 45%).

¹H NMR (400 MHz, CD₂Cl₂) δ 8.30 (s, 2H), 8.04 (s, 1H), 7.91 (m, 2H), 7.80 (d, *J* = 8.0 Hz, 1H), 7.64 (d, *J* = 4.0 Hz, 2H), 7.59 (t, *J* = 8.0 Hz, 1H), 7.45 (t, *J* = 8.0 Hz, 1H), 7.36 (d, *J* = 8.0 Hz, 1H), 7.32-7.28 (m, 1H), 4.75 (s, 2H). ¹³C NMR (101 MHz, CD₂Cl₂) δ 148.27, 141.93, 140.01, 137.62, 136.38, 134.78 (q, *J* = 32.3 Hz), 133.96, 131.95, 131.91 (q, *J* = 34.3 Hz), 129.52, 128.95, 128.65, 127.59, 126.65, 126.25, 126.24, 125.91, 124.21 (q, *J* = 276.7 Hz), 123.53 (q, *J* = 272.7 Hz), 38.34. ¹¹B NMR (128 MHz, CD₂Cl₂) δ 58.7. HR-ESIMS (*m/z*): [*M* + *H*]⁺ calcd. for C₂₆H₁₄BF₉, 509.1118; found: 509.1042.

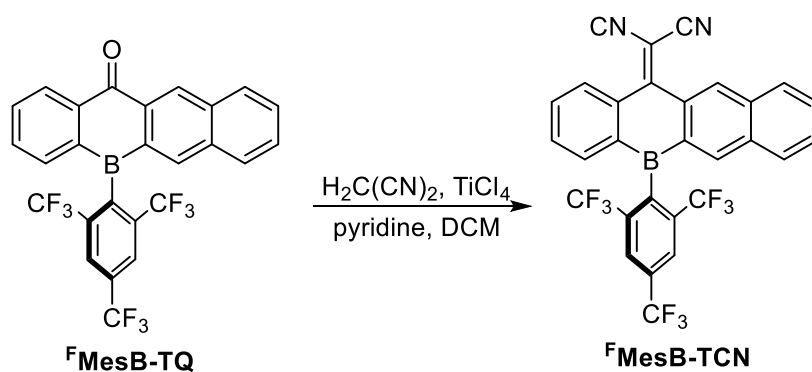
Synthesis of 5-(2,4,6-tris(trifluoromethyl)phenyl)benzo[*b*]naphtho[2,3-*e*]borinin-12(5*H*)-one (^FMesB-TQ)



To a solution of ^FMesB-T (0.50 g, 0.98 mmol) in acetic acid (35 mL) was added chromium(VI) oxide (0.26 g, 2.55 mmol). The mixture was refluxed with stirring for 12 h. After addition of water, the mixture was extracted with dichloromethane three times. The combined organic extract was washed with a saturated aqueous solution of NaHCO₃ and dried over Na₂SO₄. After filtration, the mixture was concentrated under reduced pressure. The crude product was purified by column chromatography on silica gel using petroleum ether / dichloromethane (1:1) as an eluent to give ^FMesB-TQ as pale yellow solid (0.37 g, 72%).

¹H NMR (400 MHz, CDCl₃) δ 8.69 (s, 1H), 8.30 (d, *J* = 8.0 Hz, 1H), 8.27 (s, 2H), 8.03 (d, *J* = 8 Hz, 1H), 7.90 (s, 1H), 7.83 (d, *J* = 8 Hz, 1H), 7.75-7.68 (m, 2H), 7.63 (t, *J* = 8.0 Hz, 1H), 7.57 (t, *J* = 8.0 Hz, 1H), 7.43 (d, *J* = 8 Hz, 1H). ¹³C NMR (101 MHz, CDCl₃) δ 187.74, 140.46, 139.56, 137.03, 136.13, 135.13, 134.90, 134.85 (q, *J* = 32.3 Hz), 134.11, 133.30, 132.46 (q, *J* = 34.3 Hz), 130.44, 130.40, 129.69, 129.66, 129.05, 128.64, 126.34, 123.72 (q, *J* = 276.7 Hz), 122.96 (q, *J* = 273.7 Hz). ¹¹B NMR (128 MHz, CDCl₃) δ 59.8. HR-ESIMS (*m/z*): [M + H]⁺ calcd. for C₂₆H₁₂BF₉O, 523.0910; found: 523.0923.

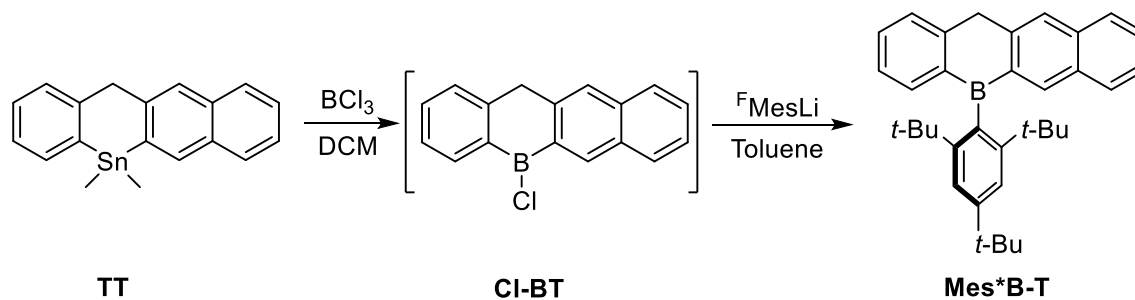
Synthesis of (*E*)-2-isocyano-2-(5-(2,4,6-tris(trifluoromethyl)phenyl)benzo[*b*]naphtho[2,3-*e*]borinin-12(5*H*)-ylidene)acetonitrile (^FMesB-TCN)



To a CH₂Cl₂ solution (15 mL) contained ^FMesB-TQ (0.35 g, 0.67 mmol) and malononitrile (53.11 mg, 0.80 mmol), TiCl₄ (2.68 mL, 2.68 mmol) was dropwise added at 0 °C in ice bath. After the mixture was stirred for 30 min, pyridine (216 μL, 2.68 mmol) was injected to stir for another 30 min. Then, the mixture was heated at 40 °C for 4 h. The reaction was quenched by water and the mixture was extracted with DCM. The collected organic layer was dried over Na₂SO₄. After filtration, the mixture was concentrated under reduced pressure. The crude product was purified by column chromatography on silica gel using petroleum ether / dichloromethane (1:1) as an eluent to give ^FMesB-TCN as white solid (0.21 g, 55%).

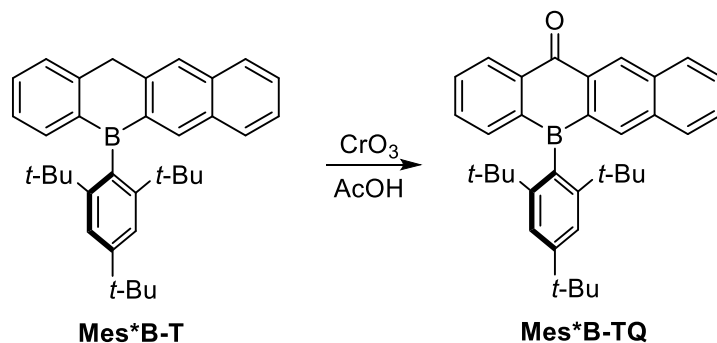
^1H NMR (400 MHz, CDCl_3) δ 8.25 (d, $J = 8.0$ Hz, 2H), 8.23 (s, 2H), 7.70 (t, $J = 8.0$ Hz, 2H), 7.56 (t, $J = 8$ Hz 2H), 7.38 (d, $J = 8$ Hz, 2H). ^{13}C NMR (101 MHz, CDCl_3) δ 169.68, 141.07, 140.22, 137.51, 137.42, 134.78 (q, $J = 32.3\text{Hz}$), 134.44, 134.09, 133.76, 132.84 (q, $J = 34.3$ Hz), 132.29, 131.96, 130.42, 129.71, 129.51, 129.47, 128.96, 127.86, 126.59, 123.72 (q, $J = 276.7$ Hz), 122.83 (q, $J = 274.7$ Hz), 114.77, 114.61, 83.29. ^{11}B NMR (128 MHz, CDCl_3) δ 59.5. HR-ESIMS (m/z): $[\text{M} + \text{H}]^+$ calcd. for $\text{C}_{29}\text{H}_{12}\text{BF}_9\text{N}_2$, 571.1023; found: 571.1042.

Synthesis of 5-(2,4,6-tri-*tert*-butylphenyl)-5,12-dihydrobenzo[*b*]naphtho[2,3-*e*]borinine (Mes*B-T)



To a stirring solution of **TT** (1.0g, 2.74 mmol) in dichloromethane at -78°C was added BCl_3 (1 M; 3.56 mL, 3.56 mmol) dropwise. The reaction mixture was allowed to slowly come to room temperature. The volatile compounds were removed under dynamic vacuum. The resultant off white solid was transferred to a sublimation vessel and the residual Me_2SnCl_2 was removed at ambient temperature under dynamic vacuum, leaving a grey solid **Cl-BT** (0.61 g, 85%). The product is extremely sensitive toward oxygen and water that should be handled accordingly. Bromo-2,4,6-tri-*tert*-butylbenzene (1.14 g, 3.5 mmol) was charged into a flame-dried Schlenk flask under nitrogen atmosphere and 20 mL of dry ether were added. The flask was cooled to -78°C and was added *n*-BuLi (1.6 M; 2.40 mL, 3.85 mmol) dropwise. The mixture was stirred at -78°C for 0.5 h and then stirred in an ice bath for another 2 h. The solvent was removed at 0°C under high vacuum, and 15 mL of dry toluene were added by syringe and the mixture was cooled to -78°C . A solution of **Cl-BT** (0.61 g, 2.32 mmol) in 20 mL dry toluene was added to the above solution, then the mixture was allowed to warm to room temperature and stirred overnight. The reaction was quenched by adding 20 mL of water. The aqueous layer was separated and extracted with dichloromethane (3×10 mL). The combined organic layers were washed with brine (20 mL), dried with Na_2SO_4 and the solvent was removed *in vacuo*. The crude product was purified by column chromatography on silica gel using petroleum ether as an eluent to give **Mes*B-T** as a white solid (0.54 g, 42%). ^1H NMR (400 MHz, CD_2Cl_2) δ 8.23 (s, 1H), 7.95 (s, 1H), 7.87 (d, $J = 8.0$ Hz, 1H), 7.81 (d, $J = 8.0$ Hz, 1H), 7.66 (d, $J = 8\text{Hz}$, 1H), 7.56 (s, 2H), 7.54 – 7.47 (m, 3H), 7.41 (t, $J = 8\text{Hz}$, 1H), 7.28 – 7.24 (m, 1H), 4.65 (s, 2H), 1.45 (s, 9H), 1.08 (s, 18H). ^{13}C NMR (101 MHz, CD_2Cl_2) δ 152.69, 148.90, 145.16, 140.71, 139.64, 138.36, 135.50, 132.26, 131.90, 129.26, 128.26, 127.86, 127.45, 126.05, 125.88, 125.41, 123.00, 119.82, 38.74, 38.36, 35.08, 34.94, 31.63. ^{11}B NMR (225 MHz, CD_2Cl_2) δ 61.0. HR-ESIMS (m/z): $[\text{M} - \text{H}]^-$ calcd. for $\text{C}_{35}\text{H}_{41}\text{B}$, 471.3217; found: 471.3231.

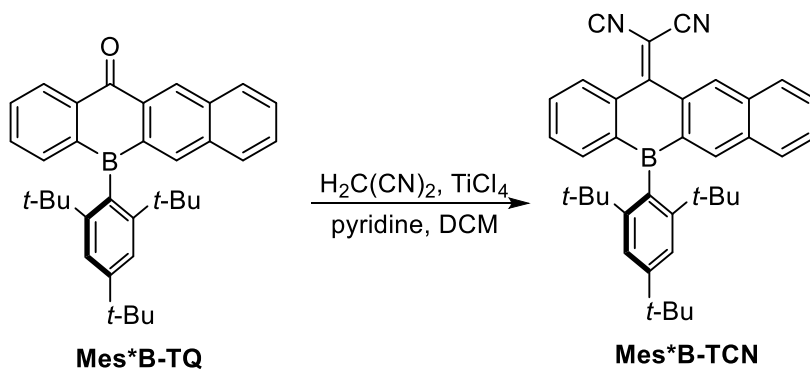
Synthesis of 5-(2,4,6-tri-*tert*-butylphenyl)benzo[*b*]naphtho[2,3-*e*]borinin-12(5*H*)-one (Mes*B-TQ)



Mes*B-TQ was obtained via similar procedure to that for ^F**MesB-TQ** as yellow solid (0.39 g, 76%).

¹H NMR (400 MHz, acetone-*d*₆) 8.97 (s, 1H), 8.46 (d, *J* = 8.0 Hz, 1H), 8.26 (d, *J* = 8.0 Hz, 2H), 8.02 (d, *J* = 8.0 Hz, 1H), 7.80 (td, *J*₁ = 7.2 Hz, *J*₂ = 1.6 Hz, 1H), 7.77 – 7.72 (m, 2H), 7.71 – 7.68 (m, 4H), 1.50 (s, 9H) 1.18 (s, 18H). ¹³C NMR (101 MHz, acetone-*d*₆) δ 187.94, 153.41, 150.04, 140.58, 138.61, 138.25, 136.22, 136.00, 134.50, 134.22, 133.75, 130.99, 130.43, 129.96, 129.79, 129.68, 128.71, 123.68, 39.09, 35.40, 35.15, 31.76. ¹¹B NMR (225 MHz, acetone-*d*₆) δ 61.4. HR-ESIMS (*m/z*): [M + H]⁺ calcd. for C₃₅H₃₉BO, 487.3167; found: 487.3171.

Synthesis of (E)-2-isocyano-2-(5-(2,4,6-tri-*tert*-butylphenyl)benzo[*b*]naphtho[2,3-*e*]borinin-12(5*H*)-ylidene)acetonitrile (Mes*B-TCN)



Mes*B-TCN was obtained via similar procedure to that for ^F**MesB-TCN** as yellow solid (0.16 g, 50%).

¹H NMR (400 MHz, CD₂Cl₂) δ 8.66 (s, 2H), 8.25 (t, *J* = 8.0 Hz, 2H), 8.04 (d, *J* = 8.0 Hz, 1H), 7.88 (d, *J* = 8 Hz, 1H), 7.80 (d, *J* = 8 Hz, 1H), 7.69 – 7.64 (m, 3H), 7.60 – 7.56 (m, 3H), 1.44 (s, 9H), 1.10 (s, 18H). ¹³C NMR (176 MHz, CD₂Cl₂) δ 171.14, 153.25, 149.86, 141.04, 138.86, 138.81, 134.76, 134.55, 134.17, 132.43, 132.08, 129.56, 129.52, 129.37, 129.31, 128.55, 127.68, 123.31, 115.46, 115.29, 82.78, 38.70, 35.12, 34.83, 31.53. ¹¹B NMR (225 MHz, CD₂Cl₂) δ 59.4. HR-ESIMS (*m/z*): [M + H]⁺ calcd. for C₃₈H₃₉BN₂, 535.3279; found: 535.3286.

3. X-ray crystallographic analyses

Single crystal samples preparation: All the single crystals were obtained via evaporation from their solution in CH₂Cl₂/Hexane mixture. The acicular crystals of ^FMesB-TCN were formed on the vial wall after slow evaporation of its solution for 1-2 days. The block crystals of ^FMesB-TCN were formed in solution after slow evaporation for 4-6 days. The block crystals of Mes*B-TCN were formed in solution after slow evaporation for 4-6 days.

Single-crystal X-ray diffraction data were collected on a Bruker D8 Venture 4-circle diffractometer using Mo/Cu- K α ($\lambda = 0.71073\text{\AA}/1.54184\text{\AA}$). The images were processed and corrected for Lorentz-polarization effects and absorption as implemented in the Bruker software packages. The structures were solved using the intrinsic phasing method (SHELXT)^[1] and Fourier expansion technique. All non-hydrogen atoms were refined in anisotropic approximation, with hydrogen atoms ‘riding’ in idealized positions, by full-matrix least squares against F^2 of all data, using SHELXL software.^[2] Hydrogen atoms were refined with isotropic displacement parameters. Olex2^[3] was used as a graphical user interface and for the preparation of the CIF files. Crystal data and experimental details are listed in Table S1-S3; full structural information have been deposited with the Cambridge Crystallographic Data Centre with deposition numbers of 2010873 (^FMesB-T), 2013631 (^FMesB-TQ), 2013632 (^FMesB-TCN, block, 180K), 2082134 (^FMesB-TCN, acicular), 2081903 (Mes*B-TCN), 2086880 (^FMesB-TCN, block, 300K), 2086881 (^FMesB-TCN, block, 400K)

Table S1 Crystal data and structure refinement for ^FMesB-T, ^FMesB-TQ, ^FMesB-TCN (Block crystal and Acicular crystal) and Mes*B-TCN.

| Identification code | ^F MesB-T | ^F MesB-TQ | ^F MesB-TCN (Block) | ^F MesB-TCN (Acicular) | Mes*B-TCN |
|----------------------------------|---|---|--|--|---|
| Empirical formula | C ₂₆ H ₁₄ BF ₉ | C ₂₆ H ₁₂ BF ₉ O | C ₂₉ H ₁₂ BF ₉ N ₂ | C ₂₉ H ₁₂ BF ₉ N ₂ | C ₃₈ H ₃₉ BN ₂ |
| Formula weight | 508.18 | 522.17 | 570.22 | 570.22 | 534.52 |
| Temperature/K | 180.0 | 180 | 180.0 | 170.00(13) | 180.0 |
| Crystal system | monoclinic | triclinic | monoclinic | monoclinic | triclinic |
| Space group | C2/c | P-1 | P2 ₁ /c | C2/c | P-1 |
| <i>a</i> /Å | 17.458(8) | 8.2738(5) | 6.8971(3) | 34.0175(5) | 8.8732(4) |
| <i>b</i> /Å | 8.246(3) | 8.7041(6) | 17.6628(7) | 10.25990(10) | 11.4960(6) |
| <i>c</i> /Å | 30.523(11) | 15.6890(10) | 20.2921(8) | 43.7874(6) | 16.2386(9) |
| α /° | 90 | 85.630(3) | 90 | 90 | 71.283(2) |
| β /° | 95.837(14) | 77.392(2) | 91.795(2) | 102.4470(10) | 77.713(2) |
| γ /° | 90 | 77.652(3) | 90 | 90 | 89.499(2) |
| Volume/Å ³ | 4371(3) | 1076.59(12) | 2470.81(18) | 14923.3(3) | 1529.73(14) |
| <i>Z</i> | 8 | 2 | 4 | 24 | 2 |
| $\rho_{\text{calc}}/\text{cm}^3$ | 1.544 | 1.611 | 1.533 | 1.523 | 1.160 |
| μ/mm^{-1} | 0.142 | 0.15 | 0.138 | 1.204 | 0.066 |
| F(000) | 2048.0 | 524 | 1144.0 | 6864 | 572.0 |

| | | | | | |
|--|--|--|--|---|--|
| Crystal size/mm ³ | 0.37 × 0.3 × 0.2 | 0.17 × 0.1 × 0.06 | 0.25 × 0.24 × 0.13 | 0.25 × 0.02 × 0.02 | 0.6 × 0.15 × 0.1 |
| Radiation | MoK α (λ = 0.71073) | MoK α (λ = 0.71073) | MoK α (λ = 0.71073) | CuK α (λ = 1.54184) | MoK α (λ = 0.71073) |
| 2 Θ range for data collection/° | 5.366 to 55.066 | 5.286 to 55.06 | 4.612 to 55.15 | 5.32 to 151.028 | 4.886 to 55.108 |
| Index ranges | -22 ≤ h ≤ 22, - 10 ≤ k ≤ 10, - 38 ≤ l ≤ 39 | -10 ≤ h ≤ 10, - 11 ≤ k ≤ 10, - 20 ≤ l ≤ 20 | -8 ≤ h ≤ 8, -22 ≤ k ≤ 22, -26 ≤ l ≤ 23 | -42 ≤ h ≤ 40, - 12 ≤ k ≤ 12, - 44 ≤ l ≤ 54 | -11 ≤ h ≤ 11, - 14 ≤ k ≤ 14, - 18 ≤ l ≤ 21 |
| Reflections collected | 24991 | 14208 | 31599 | 59715 | 18561 |
| Independent reflections | 5027 [R _{int} = 0.0479, R _{sigma} = 0.0441] | 4936 [R _{int} = 0.0427, R _{sigma} = 0.0595] | 5681 [R _{int} = 0.0486, R _{sigma} = 0.0415] | 14702 [R _{int} = 0.0468, R _{sigma} = 0.0386] | 7019 [R _{int} = 0.0474, R _{sigma} = 0.0678] |
| Data/restraints/parameters | 5027/93/353 | 4936/93/362 | 5681/93/398 | 14702/0/1136 | 7019/0/379 |
| Goodness-of-fit on F ² | 1.029 | 1.058 | 1.037 | 1.044 | 1.039 |
| Final R indexes [I ≥ 2 σ (I)] | R ₁ = 0.0545, wR ₂ = 0.1333 | R ₁ = 0.0546, wR ₂ = 0.1265 | R ₁ = 0.0441, wR ₂ = 0.1022 | R ₁ = 0.0613, wR ₂ = 0.1611 | R ₁ = 0.0553, wR ₂ = 0.1307 |
| Final R indexes [all data] | R ₁ = 0.0963, wR ₂ = 0.1549 | R ₁ = 0.1098, wR ₂ = 0.1475 | R ₁ = 0.0769, wR ₂ = 0.1172 | R ₁ = 0.0901, wR ₂ = 0.1808 | R ₁ = 0.1052, wR ₂ = 0.1518 |
| Largest diff. peak/hole / e Å ⁻³ | 0.48/-0.32 | 0.48/-0.37 | 0.25/-0.27 | 0.69/-0.56 | 0.42/-0.23 |

Table S2 Crystal data and structure refinement for block crystal of ^FMesB-TCN at 300K and 400K

| Identification code | ^F MesB-TCN (300K) | ^F MesB-TCN (400K) |
|---------------------------------------|--|--|
| CCDC number | 2086880 | 2086881 |
| Empirical formula | C ₂₉ H ₁₂ BF ₉ N ₂ | C ₂₉ H ₁₂ BF ₉ N ₂ |
| Formula weight | 570.22 | 570.22 |
| Temperature/K | 299.99(13) | 400 |
| Crystal system | monoclinic | monoclinic |
| Space group | P21/c | P21/c |
| a/Å | 7.0142(3) | 7.1478(4) |
| b/Å | 17.7383(6) | 17.7447(10) |
| c/Å | 20.3579(6) | 20.4230(16) |
| α /° | 90 | 90 |
| β /° | 91.096(3) | 83 |
| γ /° | 90 | 90 |
| Volume/Å ³ | 2532.47(16) | 2571.1(3) |
| Z | 4 | 4 |
| ρ_{calc} /cm ³ | 1.496 | 1.473 |
| μ /mm ⁻¹ | 1.182 | 1.164 |
| F(000) | 1144 | 1144 |

| | | |
|---|--|--|
| Crystal size/mm ³ | 0.15 × 0.12 × 0.1 | 0.140 × 0.130 × 0.130 |
| Radiation | CuKα (λ = 1.54184) | CuKα (λ = 1.54184) |
| 2θ range for data collection/° | 8.688 to 152.574 | 9.97 to 171.568 |
| Index ranges | -6 ≤ h ≤ 8, -21 ≤ k ≤ 20, -25 ≤ l ≤ 23 | -8 ≤ h ≤ 8, -19 ≤ k ≤ 21, -24 ≤ l ≤ 23 |
| Reflections collected | 13805 | 10115 |
| Independent reflections | 5124 [Rint = 0.0423, Rsigma = 0.0496] | 4773 [Rint = 0.0260, Rsigma = 0.0340] |
| Data/restraints/parameters | 5124/93/398 | 4773/73/426 |
| Goodness-of-fit on F ² | 1.029 | 0.878 |
| Final R indexes [I ≥ 2σ (I)] | R1 = 0.0548, wR2 = 0.1293 | R1 = 0.0647, wR2 = 0.1458 |
| Final R indexes [all data] | R1 = 0.1004, wR2 = 0.1608 | R1 = 0.0919, wR2 = 0.1570 |
| Largest diff. peak/hole / e Å ⁻³ | 0.28/-0.24 | 0.46/-0.27 |

Table S3 Selected bond lengths [Å] and angles [°] of ^FMesB-TCN(block and acicular) and Mes*B-TCN.

| Compound | a | b | c | d |
|-------------------------------------|-----------------|-----------------------------------|------------------------------|-------|
| ^F MesB-TCN (Block) | B1-C21 1.598(2) | B1-C1 1.550(3) B1-C17 1.533(2) | B1-F1 2.510 B1-F4 2.645 | 28.76 |
| | | B1-C1 1.551(4) 1.554(4) | B1-F1 2.526(4) 2.424(3) | |
| ^F MesB-TCN (Acicular) | B1-C21 1.595(4) | 1.550(4) | 2.468(4) | 23.58 |
| | 1.594(4) | B1-C17 1.539(4) | B1-F9 2.522(4) | 34.31 |
| | 1.599(4) | 1.545(4) | 2.588(3) | 26.87 |
| | | 1.545(4) | 2.686(8) | |
| Mes*B-TCN | B1-C21 1.584(2) | B1-C1 1.573(3) B1-C17 1.555(2) | B1-C30 2.733 B1-C34 2.853 | 26.20 |

a. The bond lengths of B-C^FMes/Mes*, b. the bond lengths of B-C_{Ar}, c. the bond lengths of B-C/F(adjacent to B), d. the dihedral angle between the two fused benzene rings

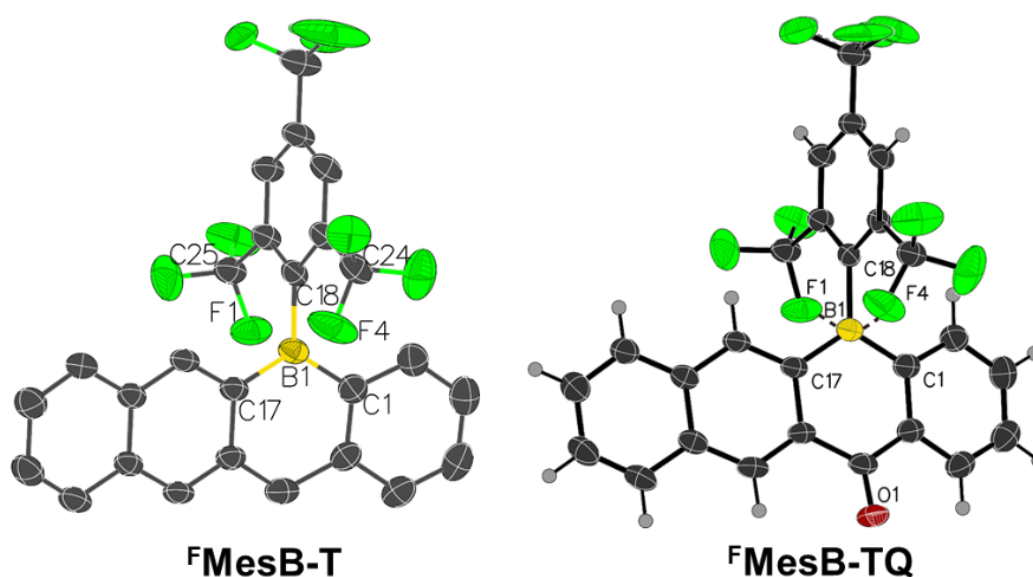


Fig. S1 Crystal structures of the methylene and carbonyl bridged triarylboranes.

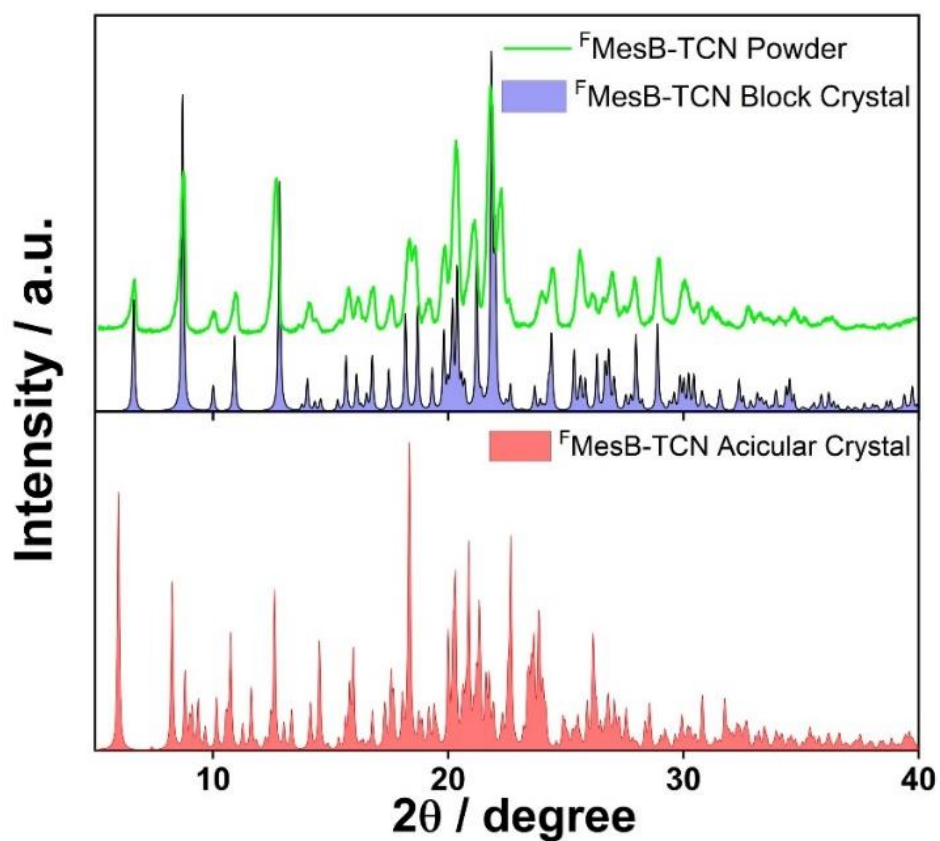


Fig. S2 XRD spectra of ^FMeSB-TCN powder* (green), block crystal (blue) and acicular crystal (red). The powder sample of ^FMeSB-TCN was obtained from rotary evaporator.

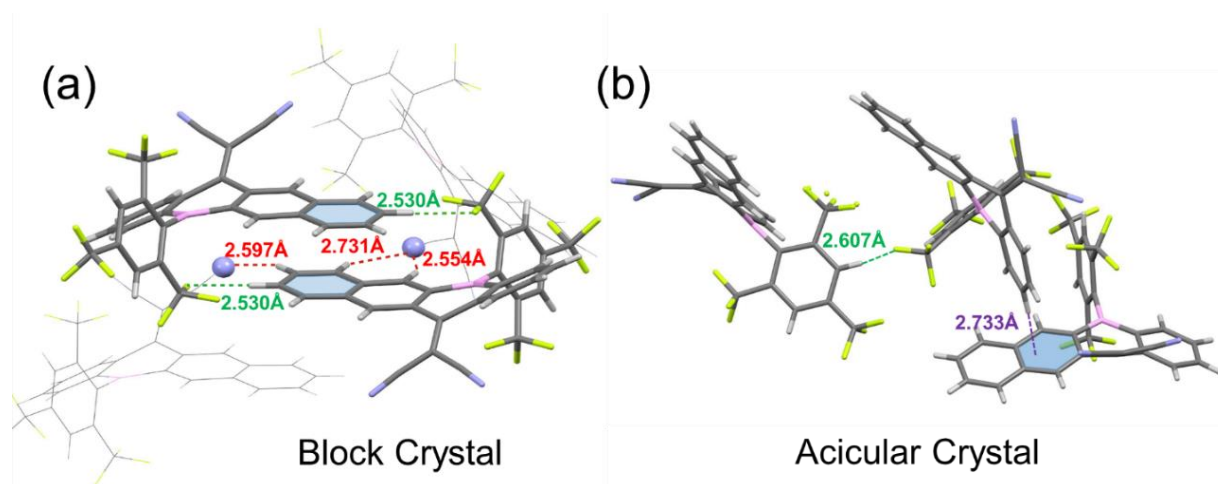


Fig. S3 Selected weak interactions in the block crystal of ^FMeSB-TCN (a) and acicular crystals (b).

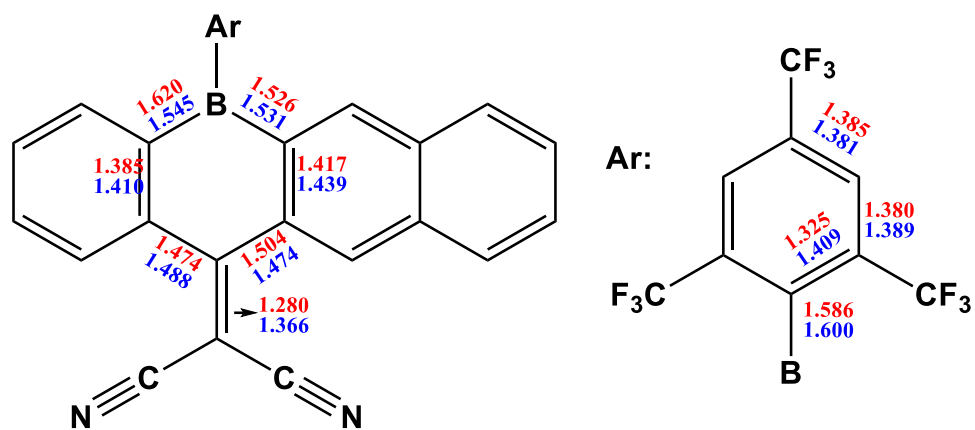


Fig. S4 Selected bond lengths in molecular structures of ^FMesB-TCN at 300K (blue) and 400K (red).

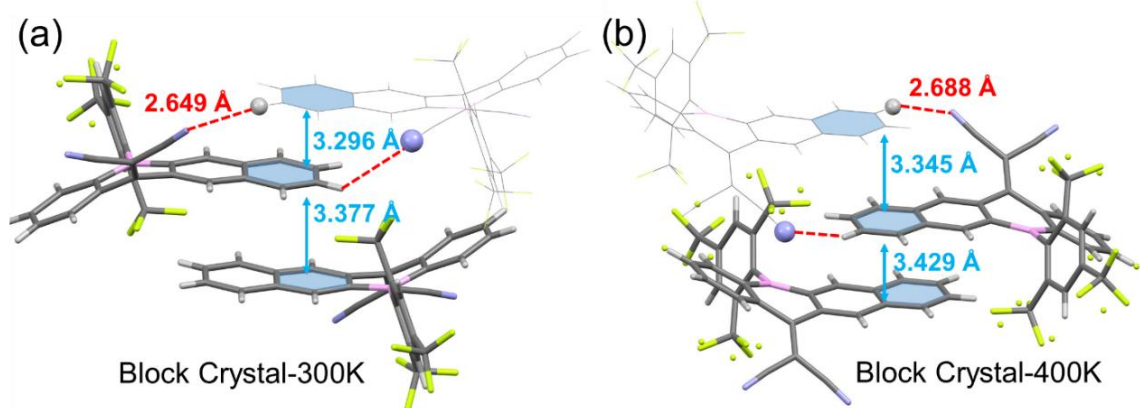


Fig. S5 Selected weak interactions in the block crystal of ^FMesB-TCN at 300 K (a) and 400K (b).

4. Photophysical and electrochemical properties

Table S4 Photophysical data of ^FMesB-TCN in different states.

| | λ_{em} (nm) | τ (ns) | Φ_F |
|------------------------------------|---------------------|-------------|------------|
| Block Crystals | 537 | 3.4 | 33% |
| Neat Film | 505 | 0.6 | 1.1% |
| Acicular Crystals | 504 | N/A | 1.3% |
| In CH ₂ Cl ₂ | 508 | N/A | 1.3% |

Table S5 Photophysical data of Mes*B-TCN in different states.

| | λ_{em} (nm) | τ (ns) | Φ_F |
|------------------------------------|---------------------|-------------|----------|
| Block Crystals | 499 | N/A | 3.8% |
| Neat Film | 505 | N/A | 1.8% |
| In CH ₂ Cl ₂ | 504 | 1.7 | 1.5% |

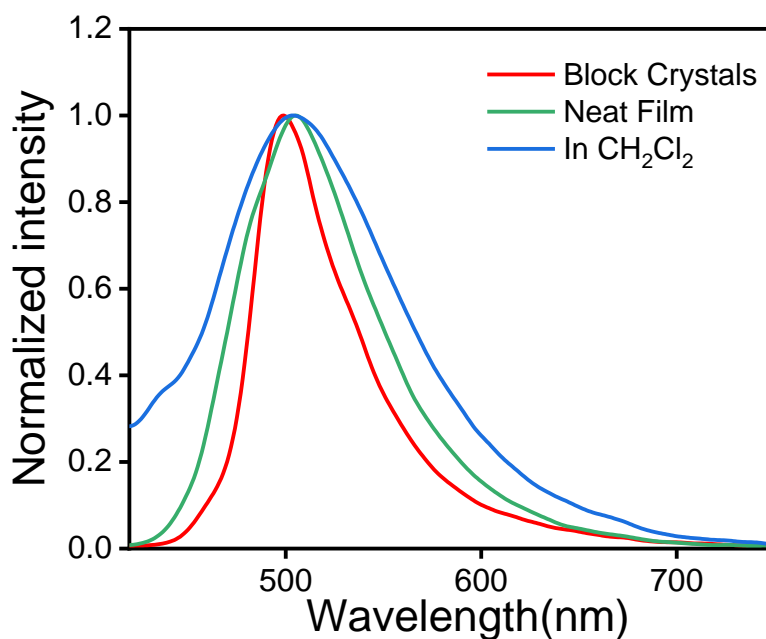


Fig. S6 PL spectra of Mes*B-TCN in different state with excitation wavelength at 400 nm.

Table S6 Electrochemical data of Mes*B-TQ, Mes*B-TCN in THF and ^FMesB-TQ, ^FMesB-TCN in CH₂Cl₂

| Compound | E_{red}^{1st} (V) ^a | E_{red}^{2nd} (V) |
|------------------------------------|----------------------------------|---------------------|
| Mes*B-TQ | -1.82 | -2.36 |
| ^F MesB-TQ | -1.62 | -2.01 |
| Mes*B-TCN | -1.33 | -1.62 |
| ^F MesB-TCN ^b | -1.19 | -1.28 |

^aAll the potentials were obtained with ferrocene as internal reference and reported versus Fc⁺⁰; ^bThe two reductive potentials of ^FMesB-TCN are obtained via Differential pulse voltammetry (DPV) because the two reductive peaks have large overlap, as shown in Fig.S7.

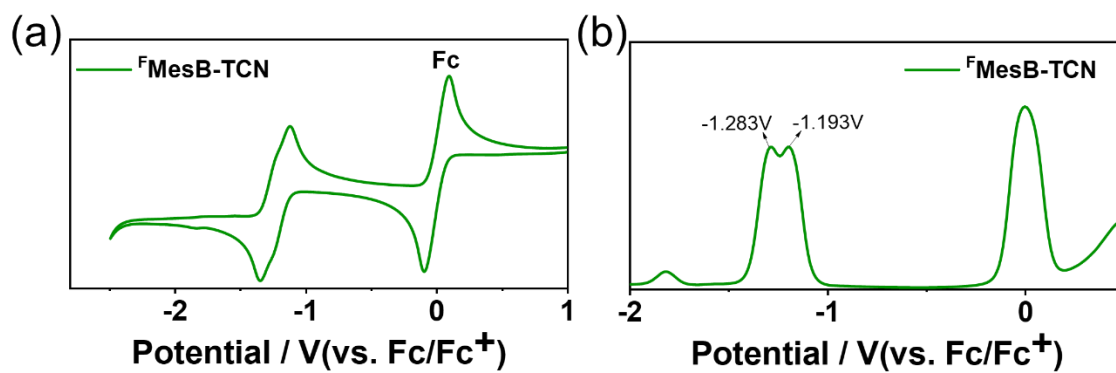


Fig. S7 (a) Cyclic-voltammetry and (b) Differential pulse voltammetry of $^{\text{F}}\text{MesB-TCN}$ in CH_2Cl_2 with ferrocene as internal reference

5. Theoretical calculations

DFT calculations of molecules in gas state were performed with the Gaussian 09 D.01 program package.^[4] Geometry optimizations were conducted at the B3LYP/6-31+G** level of theory, and single point energies were calculated at the B3PW91/6-311+G* level of theory. Vertical transitions were calculated using TD-DFT (PBE0/6-311+G**).

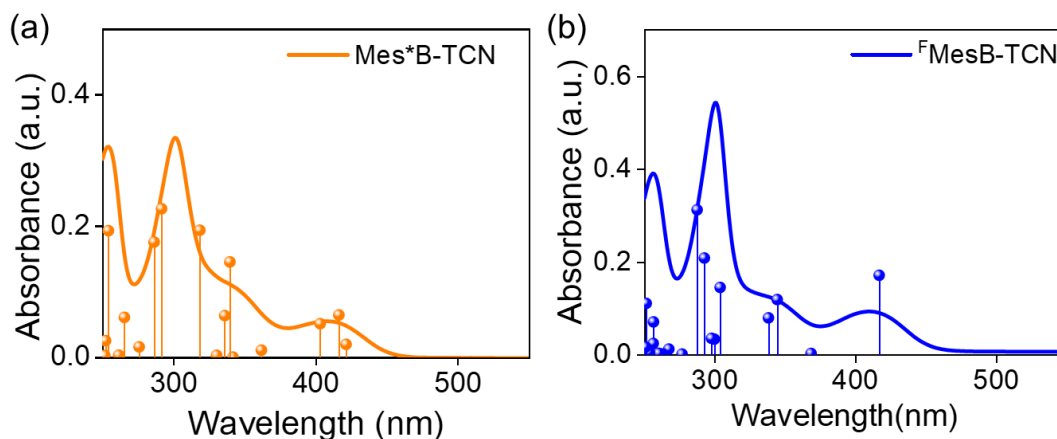


Fig. S8 UV-Vis absorption spectra of (a) **Mes*B-TCN** and (b) **^FMesB-TCN** in CH_2Cl_2 ($1 \times 10^{-5}\text{M}$), droplines are TD-DFT data at PBE0/6-311+G* level of theory.

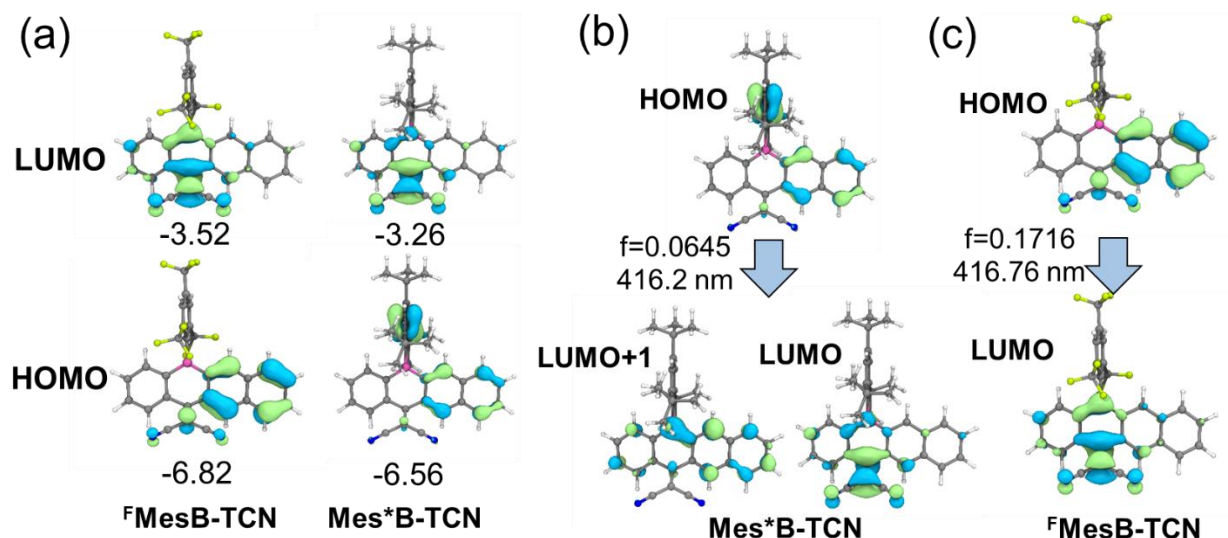


Fig. S9 (a) Plots of frontier orbitals (HOMO, LUMO) of **^FMesB-TCN** and **Mes*B-TCN**; Illustration of transition of (b) **Mes*B-TCN** and (c) **^FMesB-TCN** via TD-DFT calculation at PBE0/6-311+G** level of theory.

Table S7 TD-DFT data of dicyanomethylene functionalized triarylboranes at PBE0/6-311+G* level of theory.

| ^FMes-TCN | | | | | | | |
|----------------------------|------------------------------|----------------|-------------|----------------|-------------------------|------------|-------------|
| λ (nm) | Oscillator strength f | Assignment | possibility | λ (nm) | Oscillator strength f | Assignment | possibility |
| 416.76 | $f=0.1716$ | H-1→L+1 | 0.02 | 297.65 | $f=0.0356$ | H-1→L+1 | 0.10 |
| | | H→L | 0.95 | | | H→L+2 | 0.33 |

| | | | | | | | |
|--------|----------|---------|------|--------|----------|---------|------|
| 368.4 | f=0.0033 | H-2→L | 0.56 | 292.54 | f=0.2085 | H→L+3 | 0.52 |
| | | H-1→L | 0.33 | | | H-3→L | 0.05 |
| | | H→L+1 | 0.09 | | | H-1→L+1 | 0.73 |
| 344.27 | f=0.1193 | H-3→L | 0.05 | | | H→L+2 | 0.09 |
| | | H-2→L | 0.12 | | | H→L+3 | 0.03 |
| | | H-1→L | 0.50 | | | H→L+5 | 0.03 |
| | | H→L+1 | 0.28 | 287.4 | f=0.3124 | H-3→L | 0.05 |
| 338.07 | f=0.0798 | H-2→L | 0.27 | | | H-2→L+1 | 0.80 |
| | | H-1→L | 0.08 | | | H→L+5 | 0.04 |
| | | H→L+1 | 0.59 | 276.71 | f=0.0018 | H-8→L | 0.02 |
| 303.79 | f=0.1454 | H-3→L | 0.74 | | | H-5→L | 0.03 |
| | | H-2→L+1 | 0.04 | | | H-4→L | 0.87 |
| | | H-1→L | 0.05 | | | H-4→L+1 | 0.04 |
| | | H-1→L+1 | 0.05 | 267.33 | f=0.0127 | H-5→L | 0.84 |
| | | H→L+2 | 0.03 | | | H-4→L | 0.03 |
| | | H→L+3 | 0.04 | | | H-3→L+1 | 0.02 |
| 299.59 | f=0.0340 | H-3→L | 0.06 | 263.01 | f=0.0021 | H-3→L+1 | 0.02 |
| | | H→L+2 | 0.52 | | | H-1→L+2 | 0.40 |
| | | H→L+3 | 0.38 | | | H-1→L+3 | 0.50 |

Mes*-TCN

| λ (nm) | Oscillator strength f | Assignment | possibility | λ (nm) | Oscillator strength f | Assignment | possibility |
|----------------|-----------------------|----------------|-----------------|----------------|-----------------------|------------|-------------|
| 421.34 | f=0.0197 | H-1→L | 0.535323 | 335.94 | f=0.0635 | H-4→L | 0.13 |
| | | H-1→L+1 | 0.033967 | | | H-3→L | 0.08 |
| | | H→L | 0.393686 | | | H-1→L+1 | 0.15 |
| 416.23 | f=0.0645 | H→L+1 | 0.39851 | | | H→L+1 | 0.58 |
| | | H→L | 0.556006 | 330.23 | f=0.0030 | H-5→L | 0.07 |
| 403.1 | f=0.0512 | H-2→L | 0.933251 | | | H-4→L | 0.03 |
| 361.7 | f=0.0108 | H-4→L | 0.659871 | | | H-2→L+1 | 0.84 |
| | | H-3→L | 0.222751 | 318.35 | f=0.1936 | H-5→L | 0.72 |
| | | H-2→L+1 | 0.037631 | | | H-3→L | 0.13 |
| H→L+1 | 0.055032 | H-2→L+1 | 0.06 | | | | |
| 341.78 | f=0.0001 | H-1→L | 0.04353 | | | H→L+1 | 0.03 |
| | | H-1→L+1 | 0.744151 | 291.46 | f=0.2265 | H-3→L+1 | 0.84 |
| | | H→L+1 | 0.177441 | | | H→L+2 | 0.02 |
| 339.5 | f=0.1454 | H-5→L | 0.138264 | | | | |
| | | H-4→L | 0.122889 | 286.2 | f=0.1757 | H-5→L | 0.03 |
| | | H-3→L | 0.515762 | | | H-4→L+1 | 0.81 |
| | | H-1→L+1 | 0.029384 | | | H-3→L+1 | 0.03 |
| H→L+1 | 0.123773 | 275.71 | f=0.0158 | | | H-17→L | 0.03 |
| | | | | | | H-6→L | 0.84 |
| | | | | | | H-6→L+1 | 0.03 |
| | | | | | | H-5→L+1 | 0.03 |

DFT calculation of CIEE property

Computational Methods. The QM/MM models of ^FMesB-TCN in both block and acicular phase were setup based on the experimental crystal structures accordingly in Gaussian 16 package.^[5] For crystal in the block phase, one central ^FMesB-TCN was set as QM region, while MM region consisting of 48 molecules; for crystal in the acicular phase, one central ^FMesB-TCN was defined as QM region, while other 72 molecules were set as the MM region (see Fig. 1). Herein we adopted (TD)PW6B95/6-31G** for ^FMesB-TCN in the QM region, the MM region was dealt with by universal force field (UFF), with the electrostatic embedding scheme for the QM/MM treatments. The electrostatic embedding scheme with QM polarization was adopted. During the geometry optimizations, all atoms in the QM molecule were allowed to move, all other molecules in MM region were kept fixed as the environment. The equilibrium geometries of S₀ and S₁ were determined at the DFT/TD-DFT level, respectively. The absence of imaginary frequencies were carefully checked for both optimized structures.

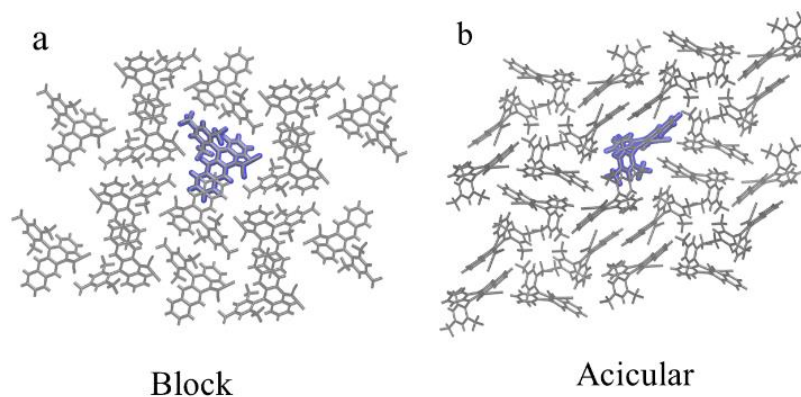


Fig. S10 QM/MM model: The molecule in the center is the QM part (blue), the remaining molecules are MM parts (grey).

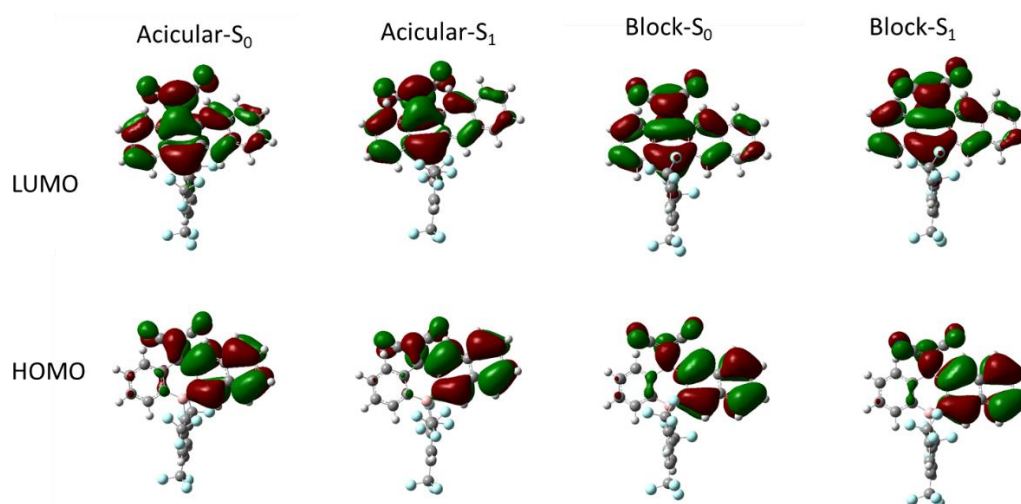


Fig. S11 Electron density contours of HOMO and LUMO for the ground state and excited state of block crystal and acicular crystal at the PW6B95/6-31G** level.

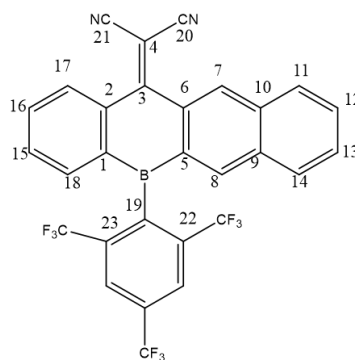
Table S8 Calculated vertical excitation energy (VEE), oscillator strength (f), and HOMO \rightarrow LUMO assignments for the block and acicular crystal.

| S_1 | VEE | Exp | EDM | f | assignment |
|------------------|---------|---------|--------|--------|-------------------------|
| block crystal | 2.55 eV | 2.31 eV | 4.20 D | 0.1710 | HOMO \rightarrow LUMO |
| acicular crystal | 2.61 eV | 2.46 eV | 4.13 D | 0.1687 | HOMO \rightarrow LUMO |

Table S9 Reorganization energies λ obtained by AP methods in both block and acicular crystal phases.

| | λ_{gs} (meV) | λ_{es} (meV) | λ_{total} (meV) |
|------------------|----------------------|----------------------|-------------------------|
| block crystal | 216 | 214 | 430 |
| acicular crystal | 211 | 239 | 450 |

Table S10 The changes of selected angles and dihedral angles of acicular and block crystal from ground state to excited state.

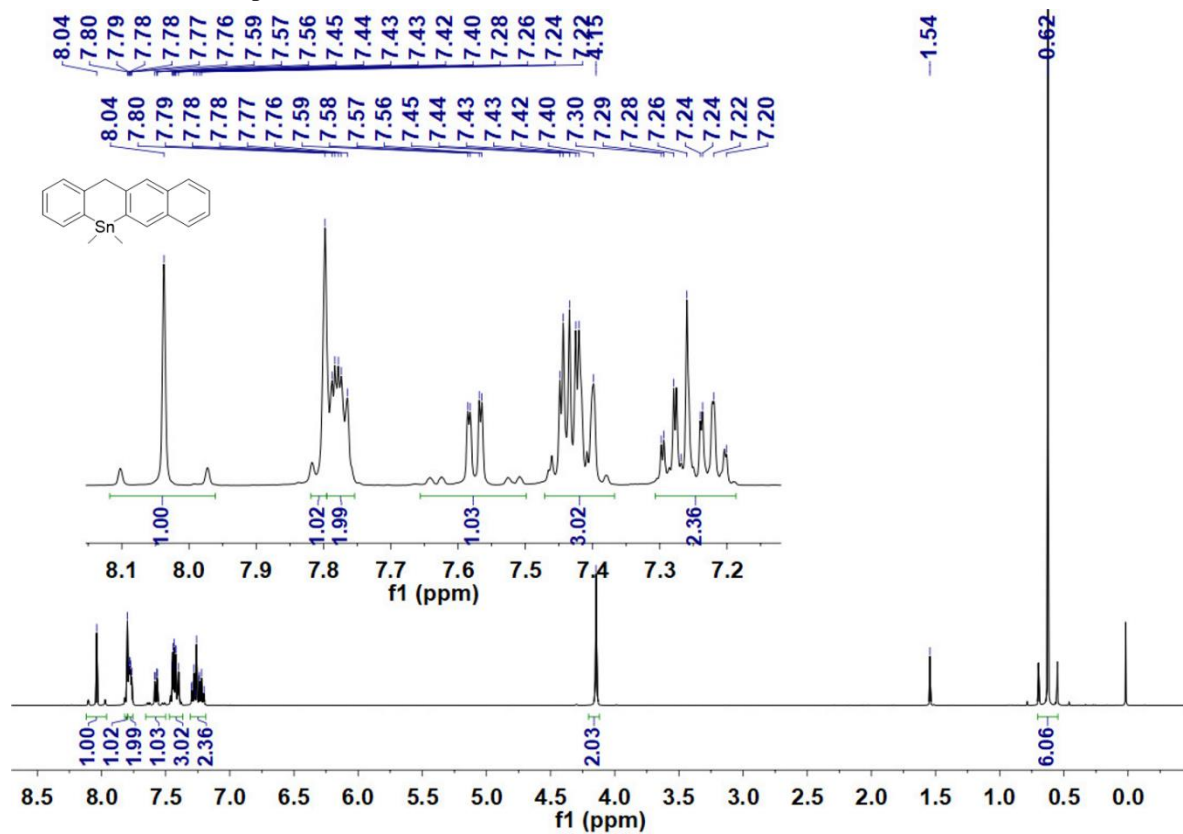


| Angles and Dihedral angles/ $^\circ$ | Acicular crystal | | | Block crystal | | |
|---|------------------|-----------|---------------------|---------------|-----------|---------------------|
| | S_0 | S_1 | $ \Delta(S_0-S_1) $ | S_0 | S_1 | $ \Delta(S_0-S_1) $ |
| C ₁ -B-C ₅ | 116.1080 | 115.5078 | 0.6002 | 116.1288 | 115.5791 | 0.5497 |
| B-C ₅ -C ₆ | 119.6961 | 119.3318 | 0.3643 | 119.7548 | 119.4788 | 0.2760 |
| C ₁₉ -B-C ₁ -C ₂ | -172.3086 | -167.7919 | 4.5167 | 172.8519 | 168.6082 | 4.2437 |
| C ₁₉ -B-C ₅ -C ₆ | 172.3294 | 169.8927 | 2.4367 | -170.4754 | -169.4606 | 1.0148 |
| C ₅ -B-C ₁₉ -C ₂₂ | -95.5722 | -92.1228 | 3.4494 | -83.5516 | -86.6066 | 3.0550 |
| C ₅ -B-C ₁₉ -C ₂₃ | 92.0836 | 96.1756 | 4.0920 | 98.2908 | 95.2005 | 3.0903 |
| C ₁ -B-C ₁₉ -C ₂₃ | -82.1070 | -81.0364 | 1.0706 | -87.3192 | -87.7527 | 0.4335 |
| C ₈ -C ₉ -C ₁₄ -C ₁₃ | -176.7387 | -175.1216 | 1.6171 | 177.0161 | 175.8149 | 1.2012 |
| C ₇ -C ₁₀ -C ₁₁ -C ₁₂ | 179.8906 | 178.2717 | 1.6189 | -179.4622 | 0.7553 | 1.2931 |

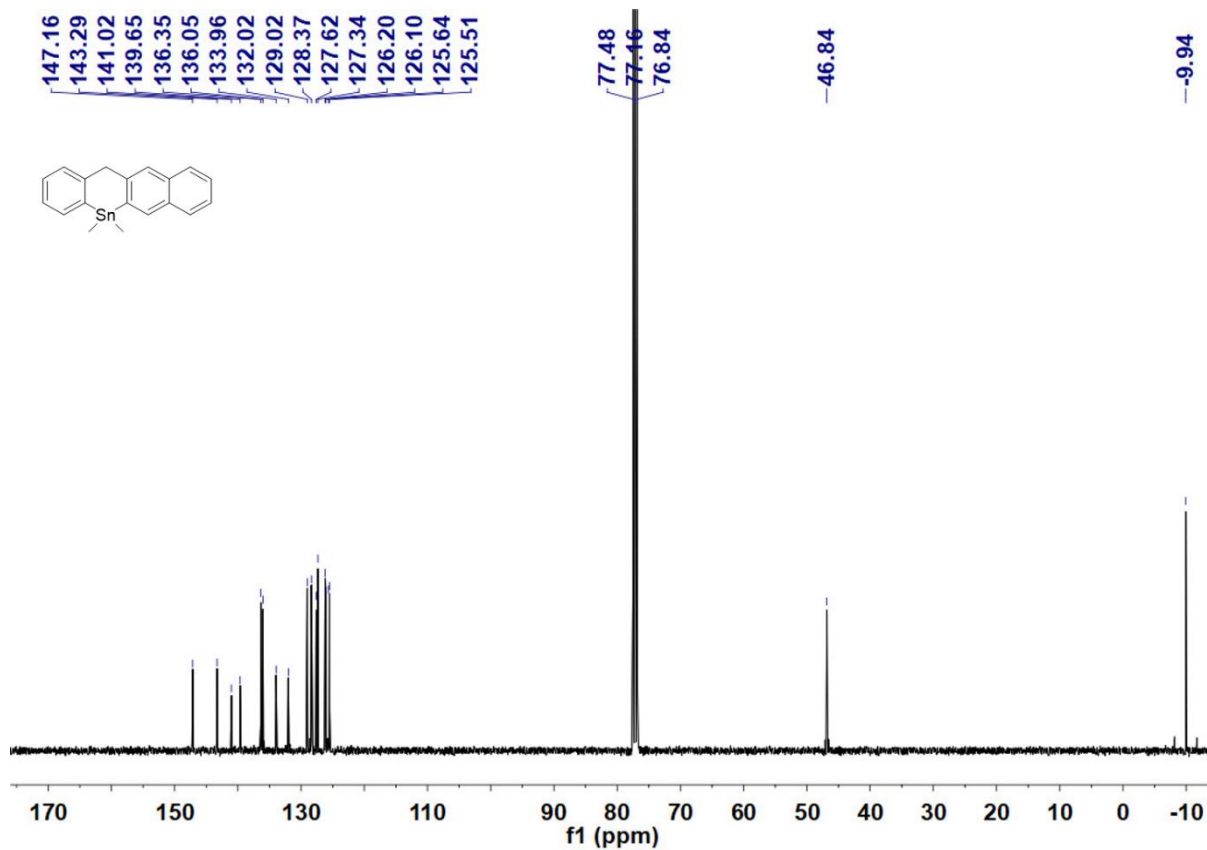
Table S11 Benchmark of different functions using UV-vis and PL spectra of ^FMesB-TCN in THF solution with Gaussian 16 soft package

| | B3LYP | BHandHLYP | CAM-B3LYP | M062X | ω B97XD | BMK | PW6B95 | Exp |
|----------------------------|--------|-----------|-----------|--------|----------------|--------|---------------|-----|
| Absorption (nstates=20) | 442.00 | 349.12 | 353.61 | 353.01 | 346.72 | 382.54 | 416.24 | 410 |
| Emission | 536.01 | 438.96 | 454.29 | 442.13 | 456.29 | 470.97 | 507.54 | 501 |

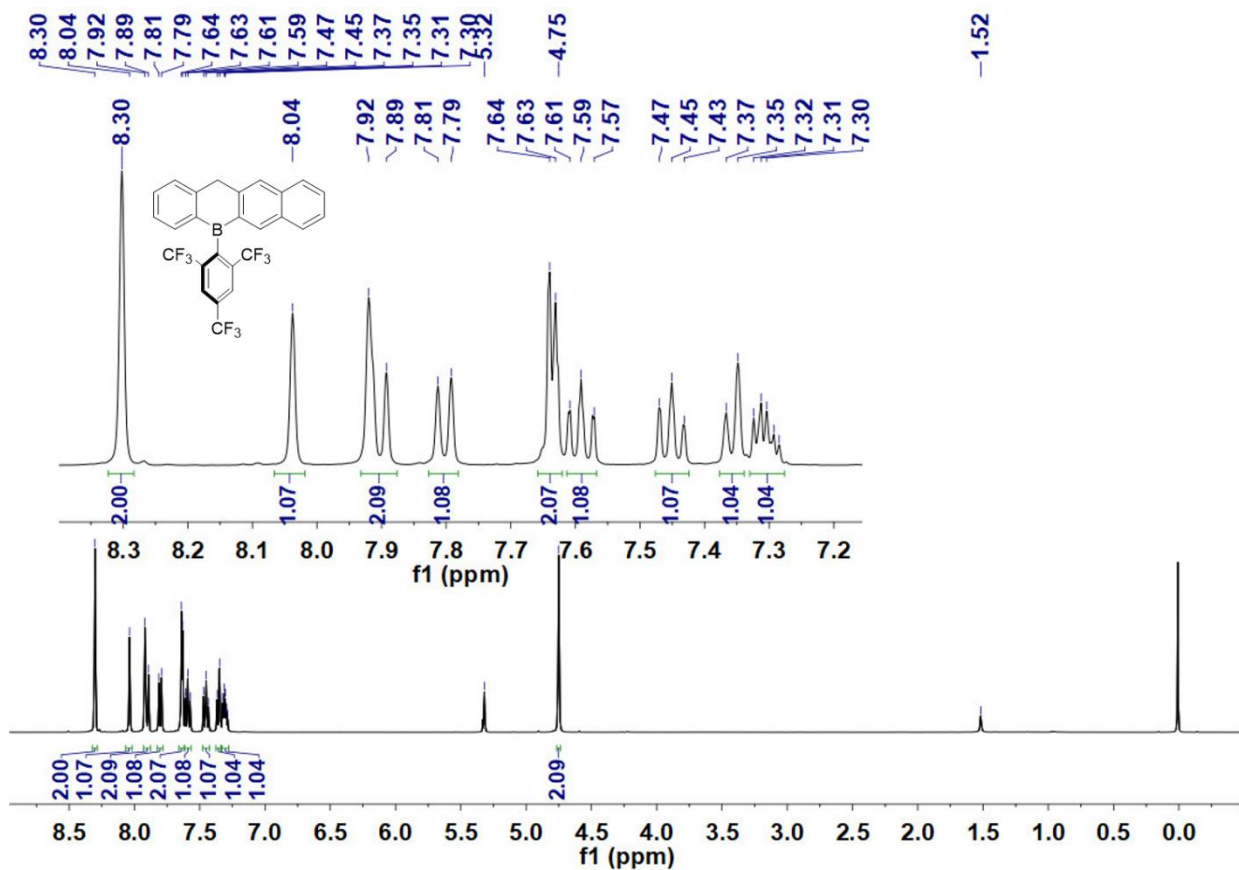
6. ^1H , ^{13}C and ^{11}B NMR spectra



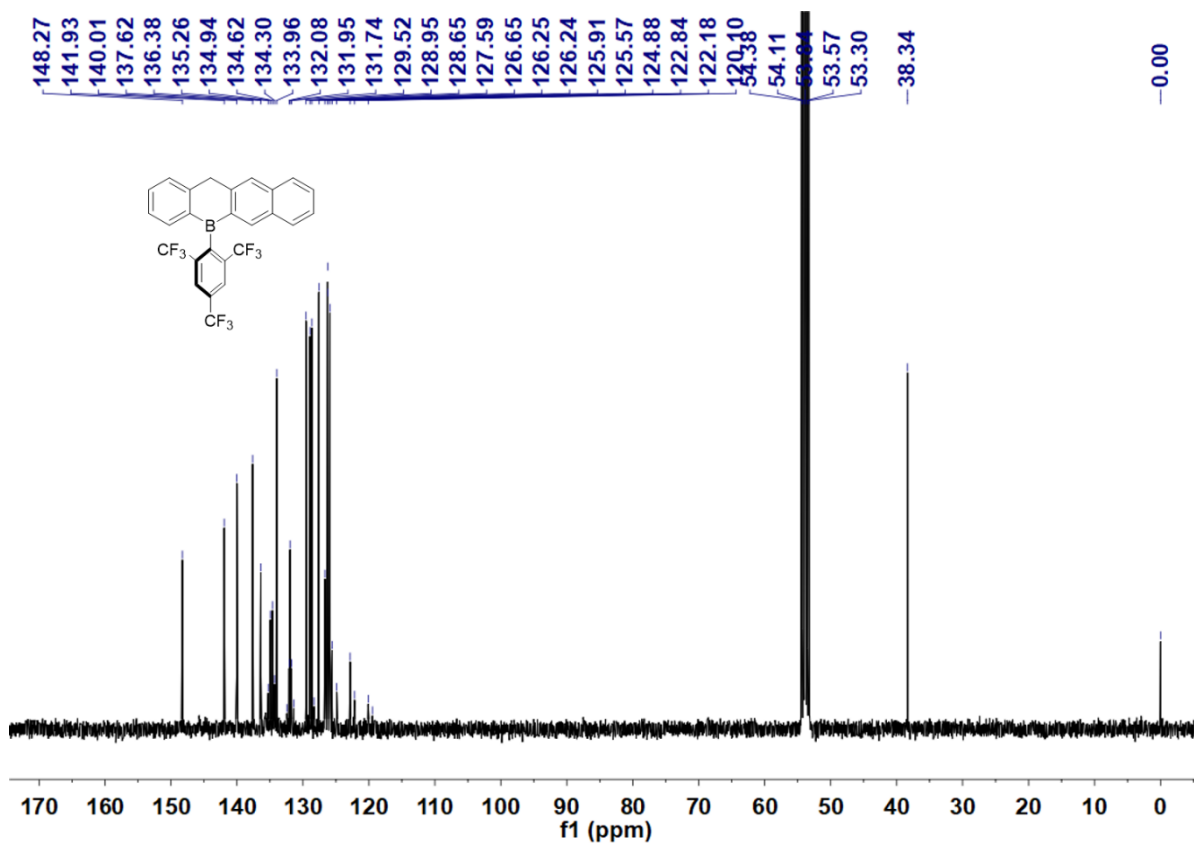
^1H NMR spectrum of TT in CDCl_3 .



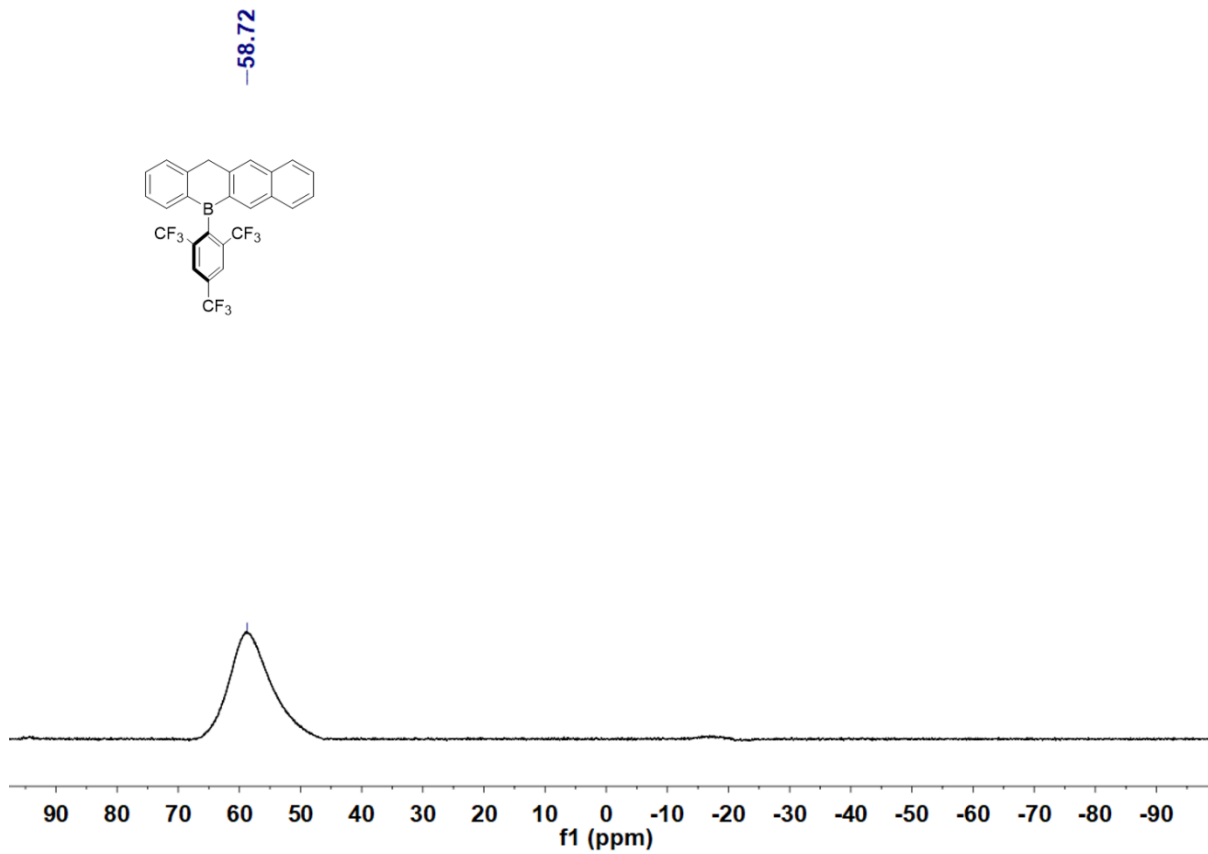
^{13}C NMR spectrum of TT in CDCl_3 .



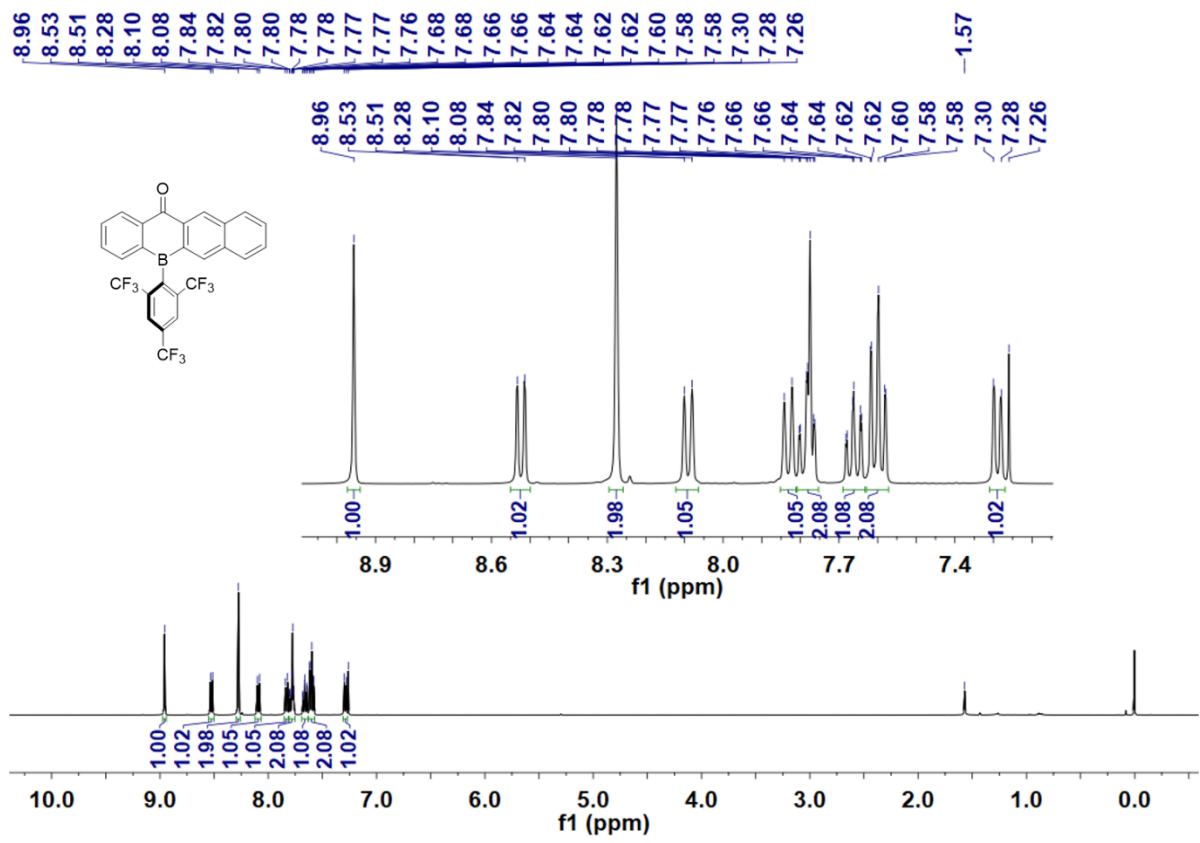
¹H NMR spectrum of ^FMesB-T in CD₂Cl₂.



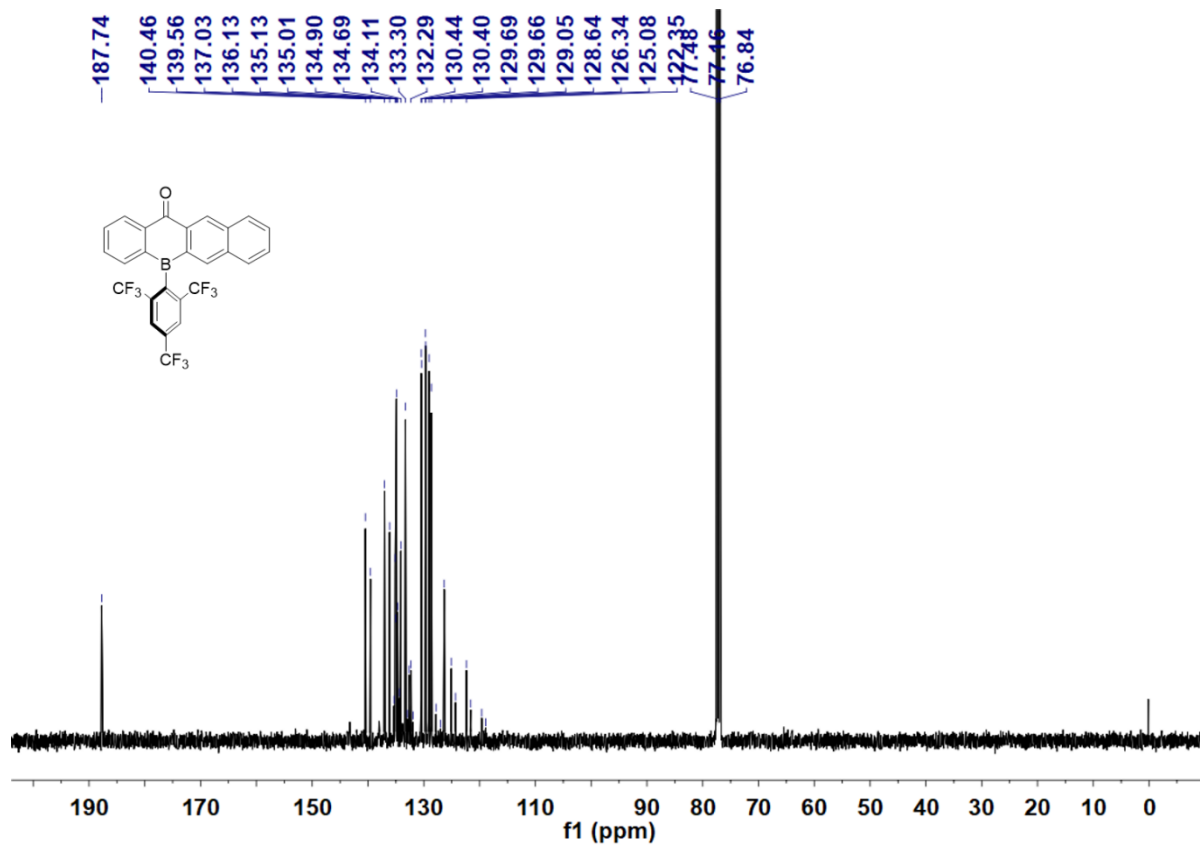
¹³C NMR spectrum of ^FMesB-T in CD₂Cl₂.



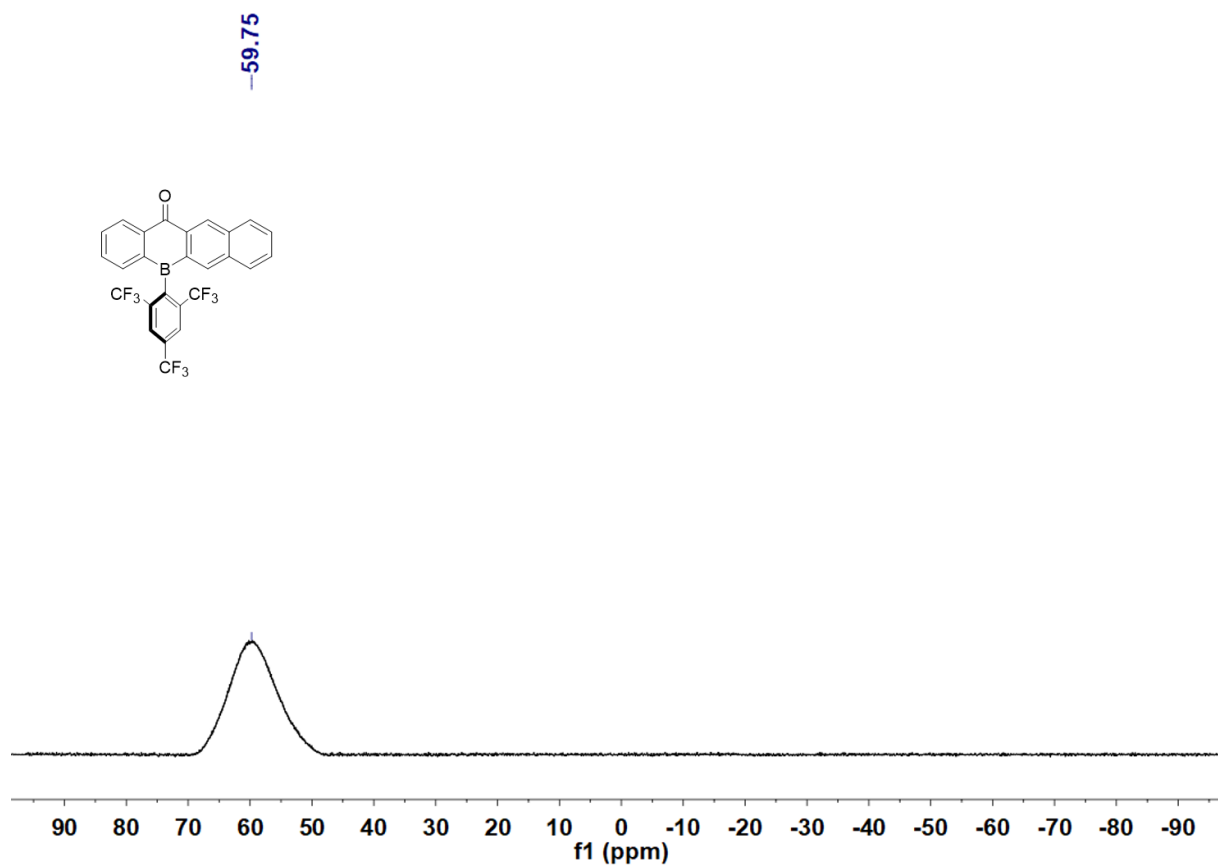
^{11}B NMR spectrum of $^{\text{F}}\text{MesB-T}$ in CD_2Cl_2 .



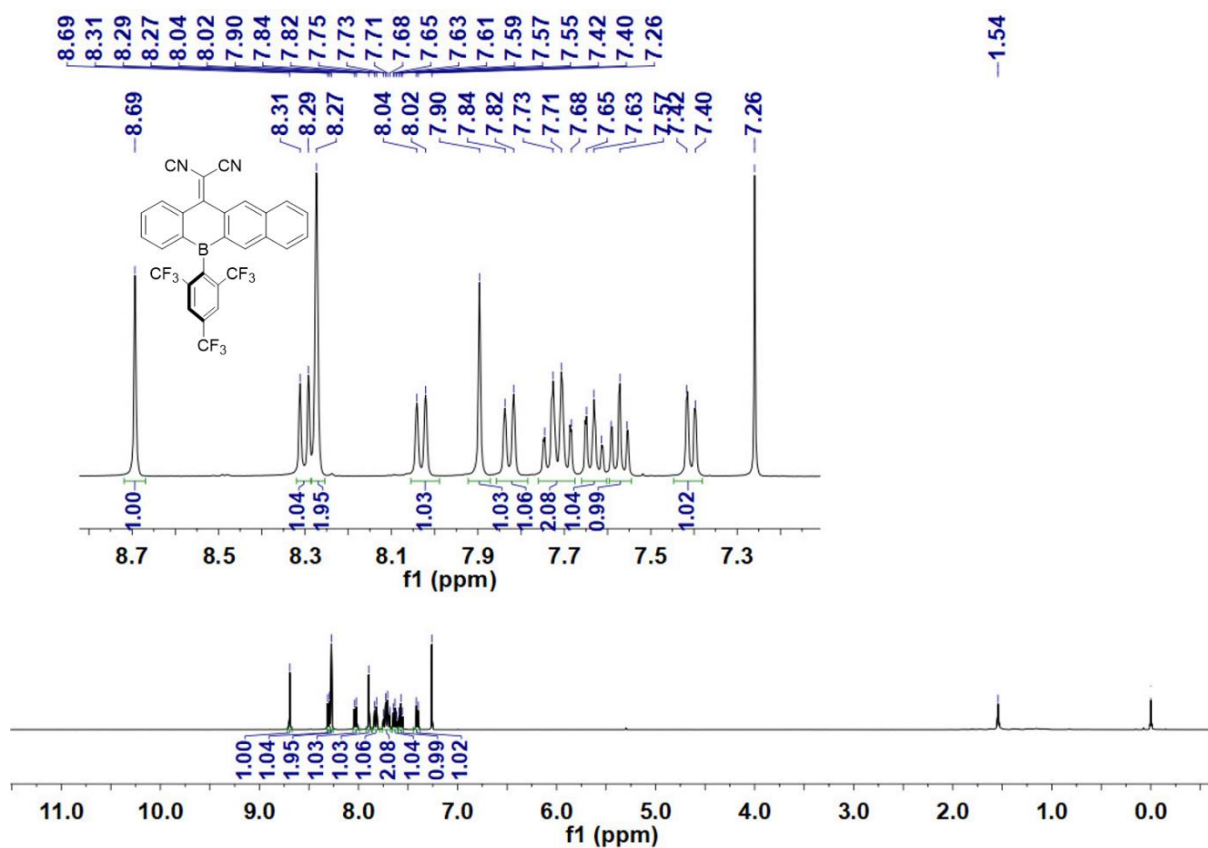
^1H NMR spectrum of $^{\text{F}}\text{MesB-TQ}$ in CDCl_3 .



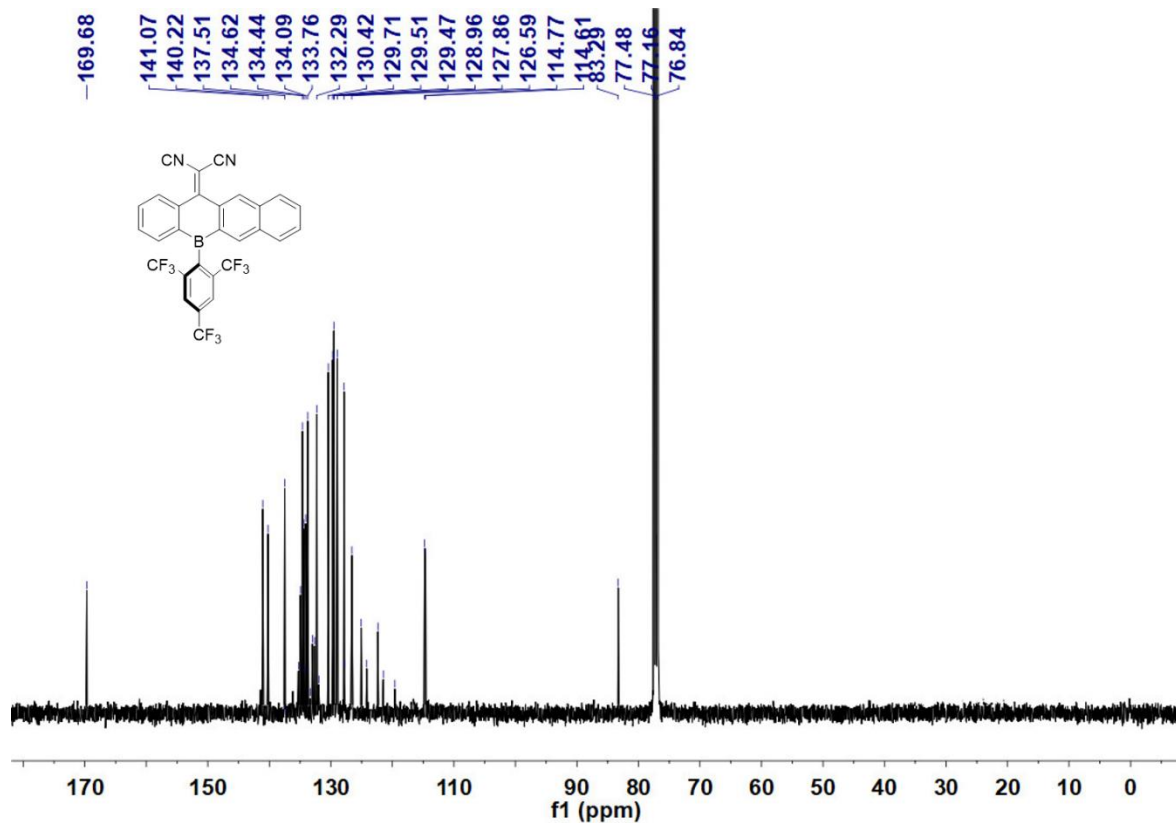
¹³C NMR spectrum of **FMeSB-TQ** in CDCl₃.



¹¹B NMR spectrum of **FMeSB-TQ** in CDCl₃.

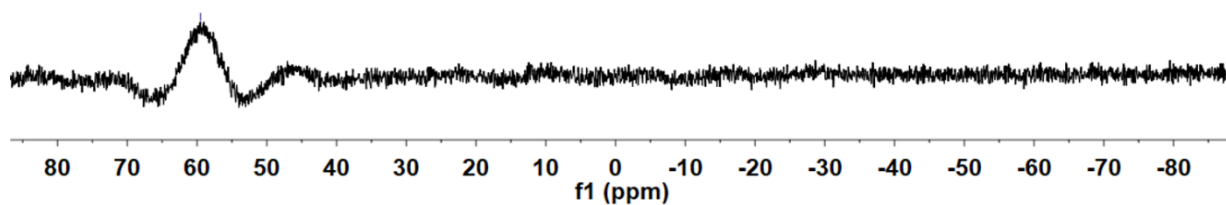
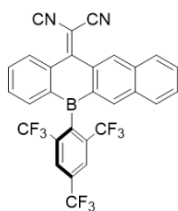


¹H NMR spectrum of ^FMesB-TCN in CDCl₃.

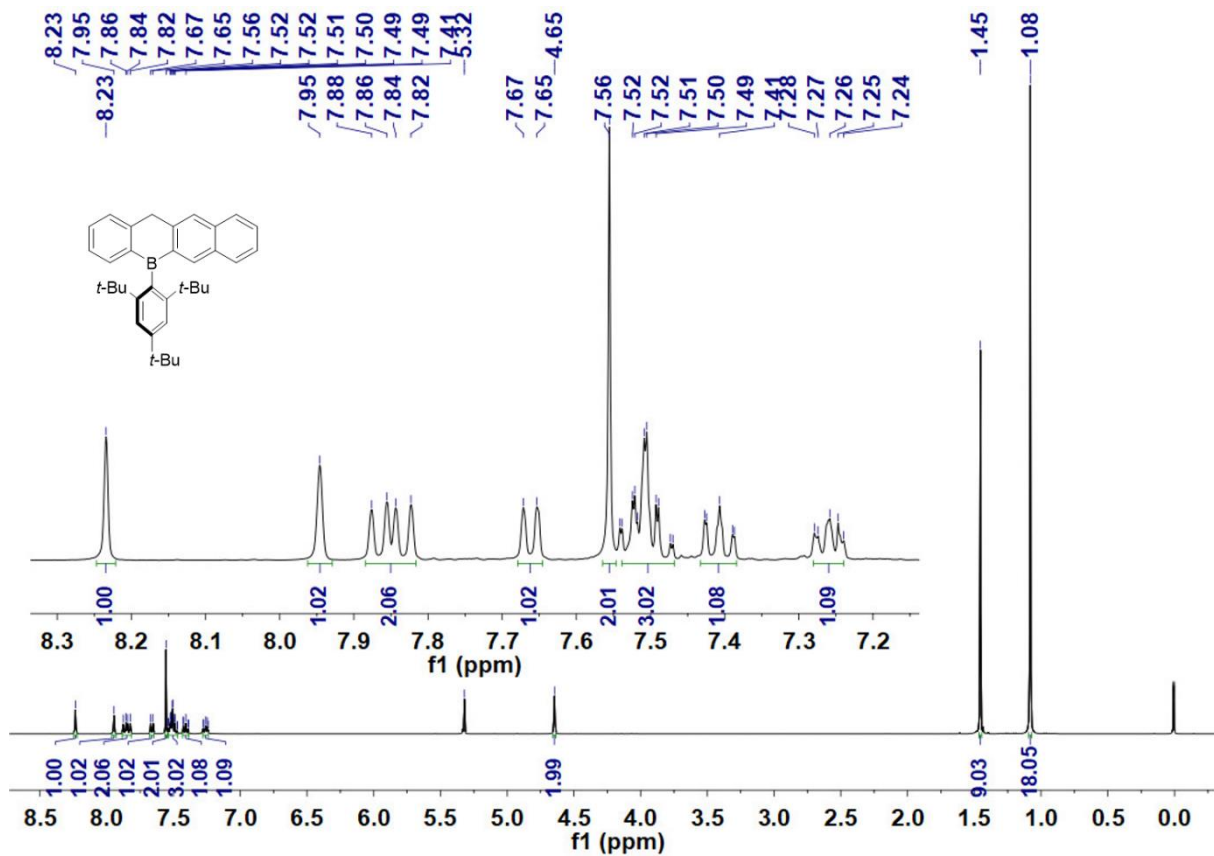


¹³C NMR spectrum of ^FMesB-TCN in CDCl₃.

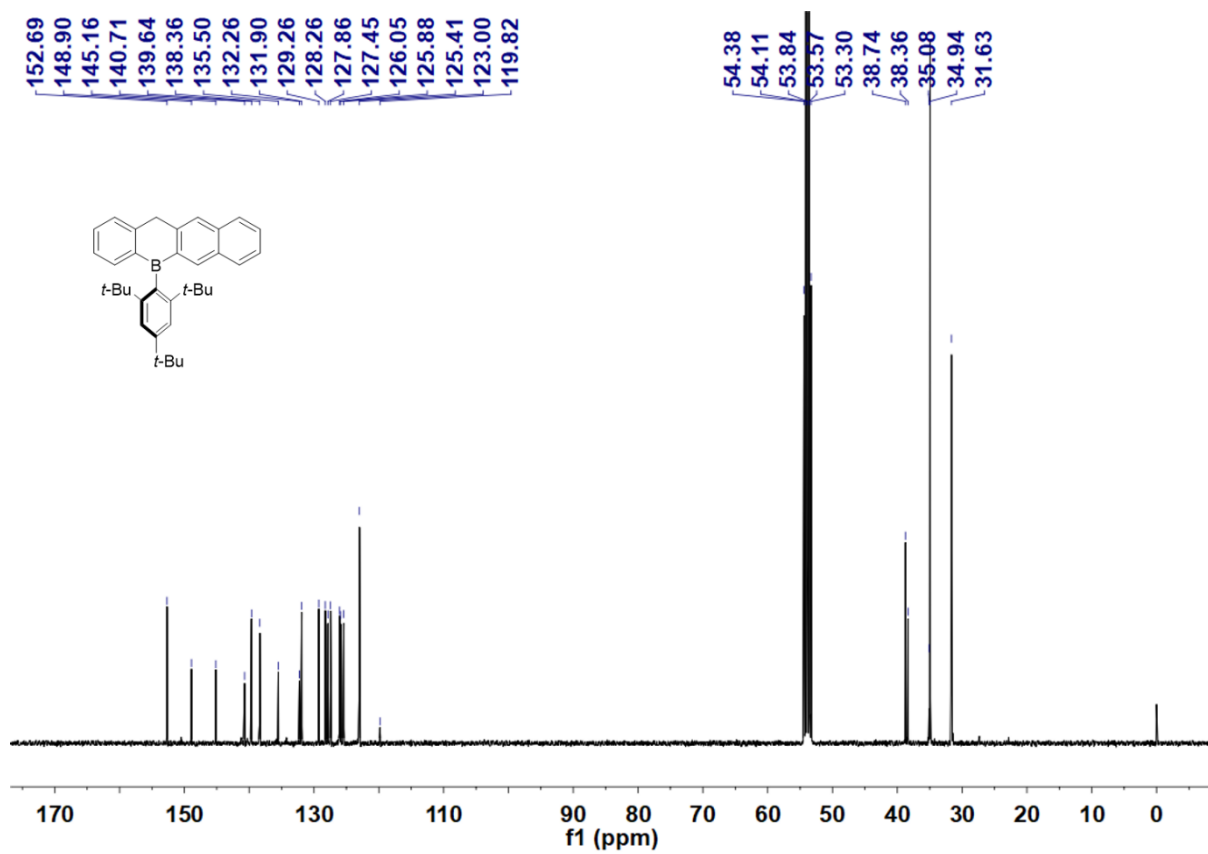
-59.51



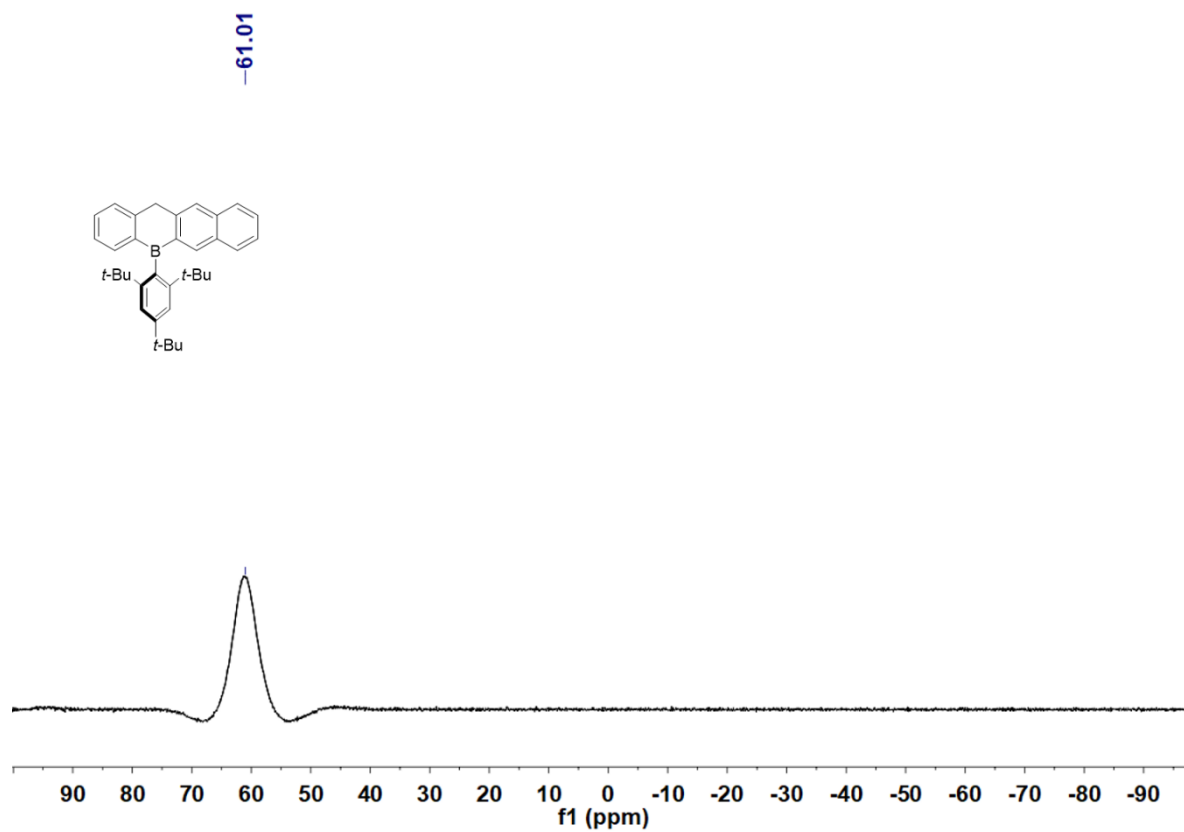
^{11}B NMR spectrum of $^{\text{F}}\text{MesB-TCN}$ in CDCl_3 .



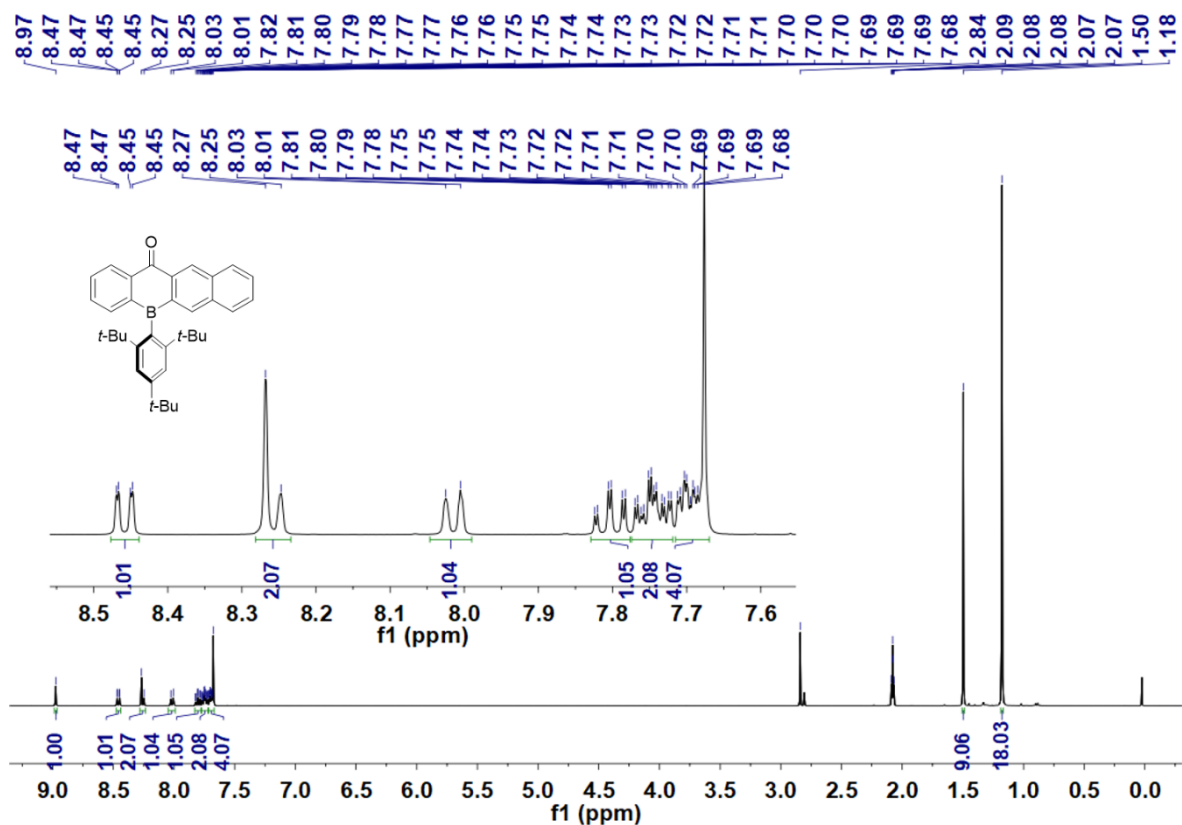
^1H NMR spectrum of $\text{Mes}^*\text{B-T}$ in CD_2Cl_2 .



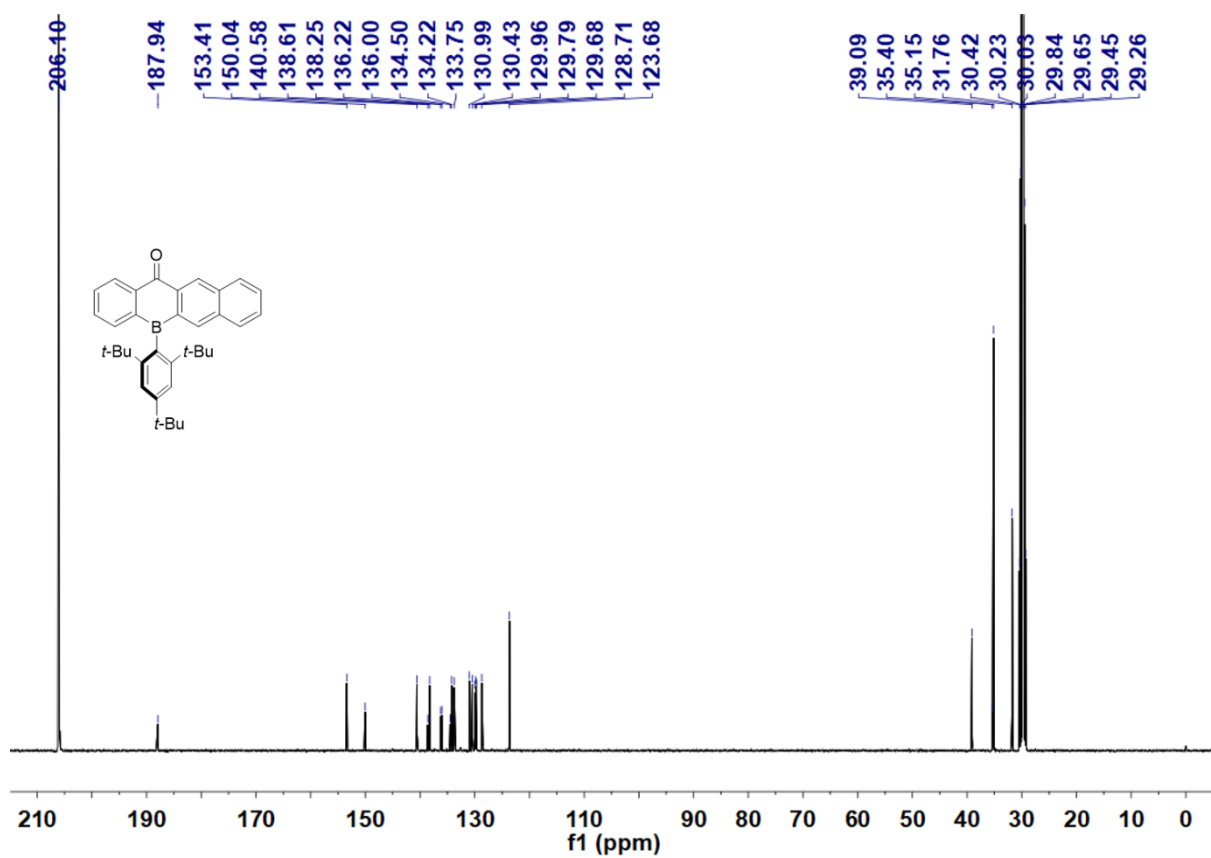
¹³C NMR spectrum of Mes*B-T in CD₂Cl₂.



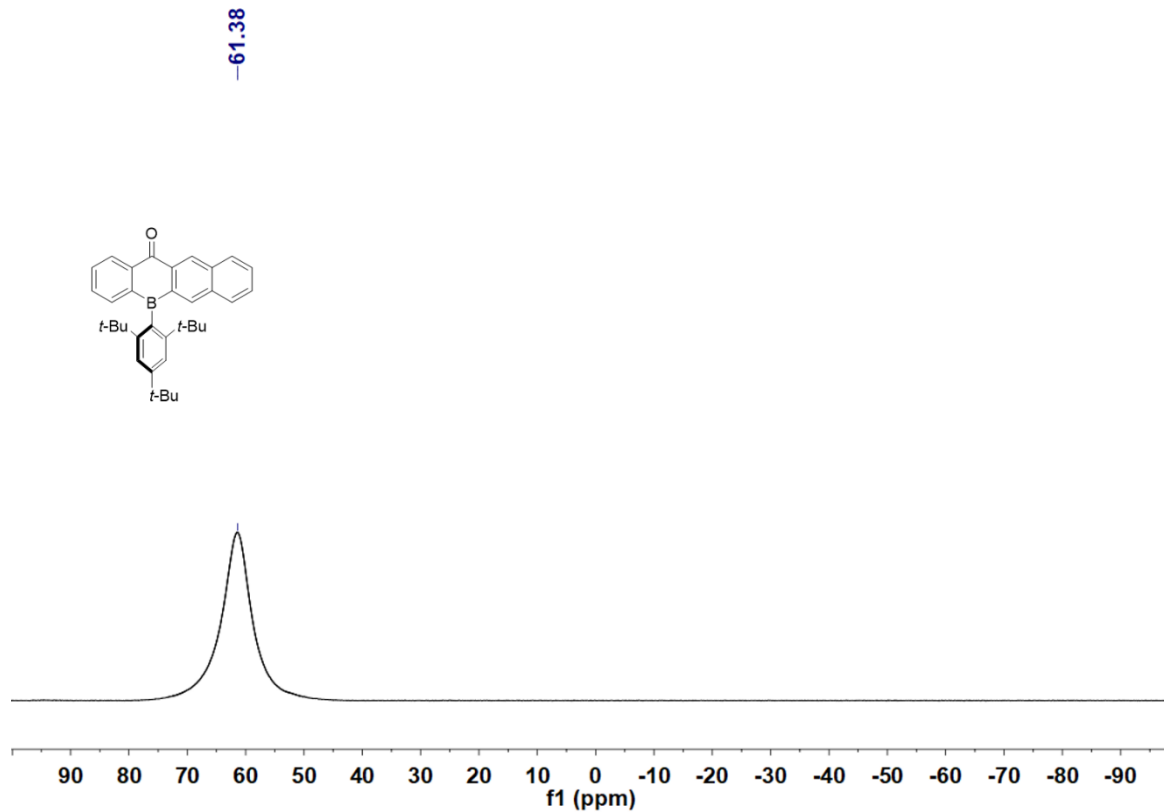
¹¹B NMR spectrum of Mes*B-T in CD₂Cl₂.



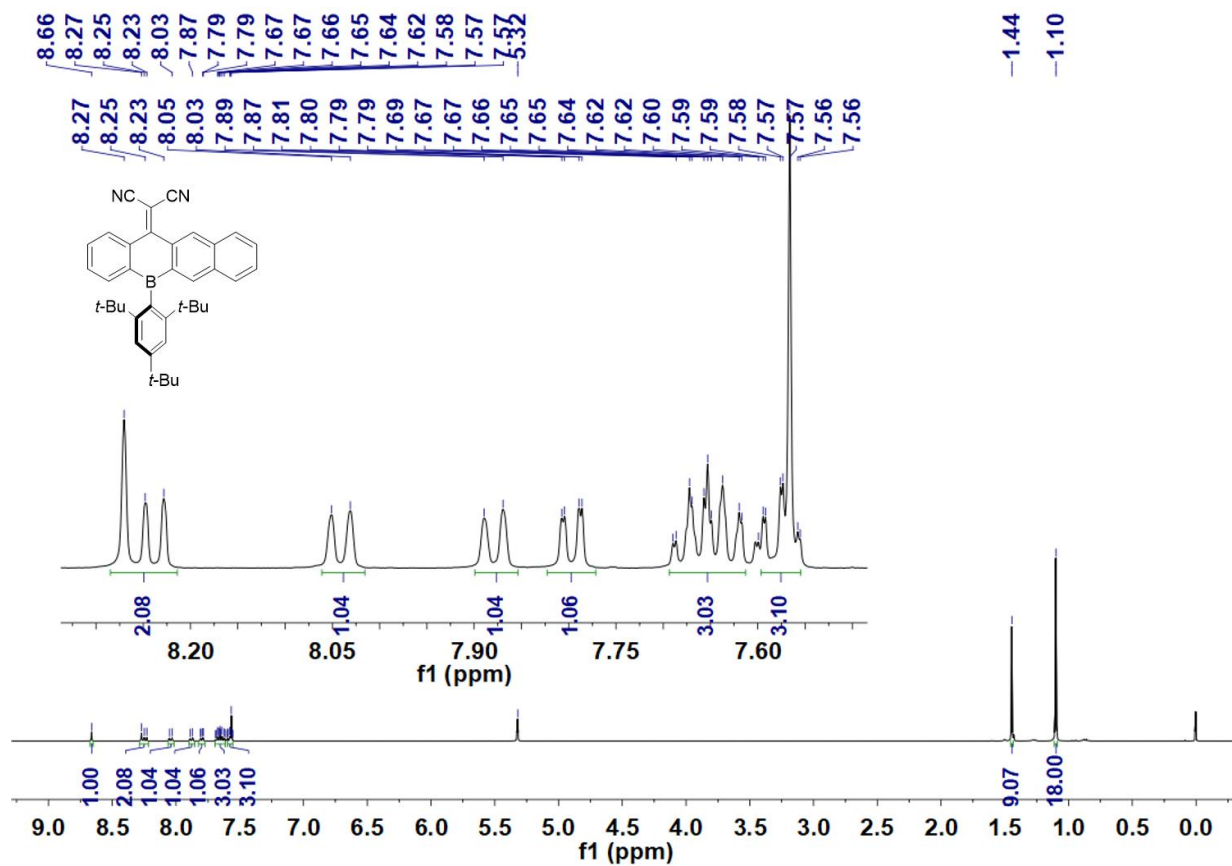
¹H NMR spectrum of Mes*B-TQ in acetone-*d*₆.



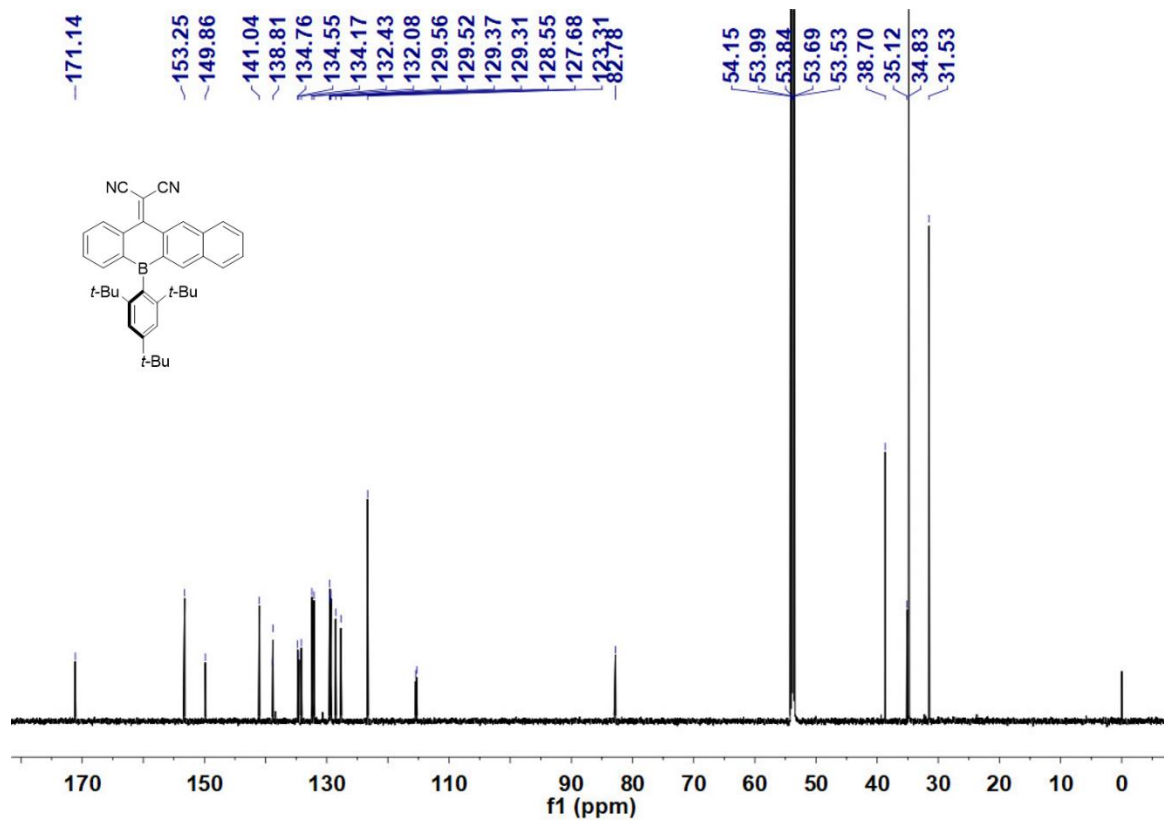
¹³C NMR spectrum of Mes*B-TQ in acetone-*d*₆.



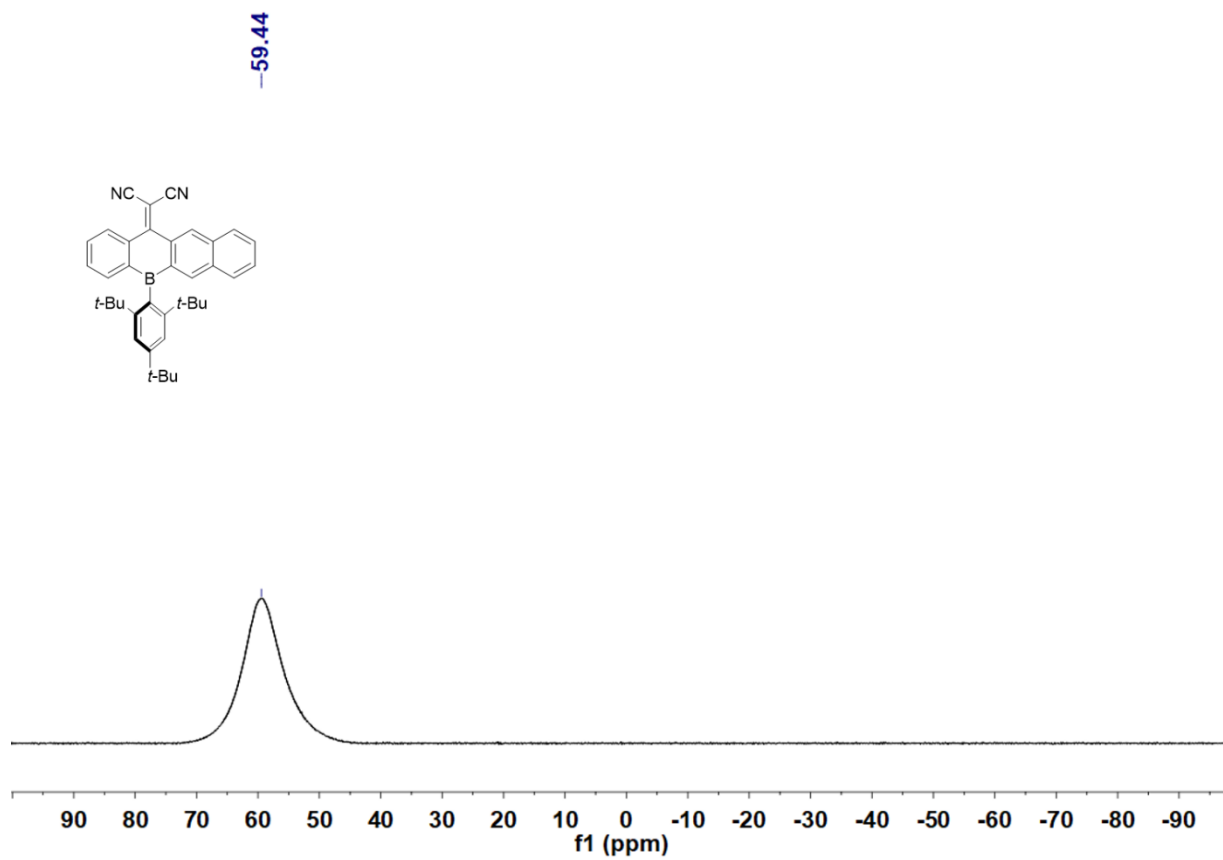
¹¹B NMR spectrum of Mes*B-TQ in acetone-*d*₆.



¹H NMR spectrum of Mes*B-TCN in CD₂Cl₂.



¹³C NMR spectrum of Mes*B-TCN in CD₂Cl₂.



¹¹B NMR spectrum of Mes*B-TCN in CD₂Cl₂.

7. Reference

- [1] G. M. Sheldrick, *Acta Crystallogr. Sect. C* **2015**, *71*, 3–8.
- [2] G. M. Sheldrick, *Acta Crystallogr. Sect. A* **2008**, *64*, 112–122.
- [3] O. V Dolomanov, L. J. Bourhis, R. J. Gildea, J. A. K. Howard, H. Puschmann, *J. Appl. Crystallogr.* **2009**, *42*, 339–341.
- [4] *Gaussian 09, Revision D.01*, M. J. Frisch, G. W. Trucks, H. B. Schlegel, G. E. Scuseria, M. A. Robb, J. R. Cheeseman, G. Scalmani, V. Barone, B. Mennucci, G. A. Petersson, H. Nakatsuji, M. Caricato, X. Li, H. P. Hratchian, A. F. Izmaylov, J. Bloino, G. Zheng, J. L. Sonnenberg, M. Hada, M. Ehara, K. Toyota, R. Fukuda, J. Hasegawa, M. Ishida, T. Nakajima, Y. Honda, O. Kitao, H. Nakai, T. Vreven, J. A. Montgomery Jr., J. E. Peralta, F. Ogliaro, M. J. Bearpark, J. Heyd, E. N. Brothers, K. N. Kudin, V. N. Staroverov, R. Kobayashi, J. Normand, K. Raghavachari, A. P. Rendell, J. C. Burant, S. S. Iyengar, J. Tomasi, M. Cossi, N. Rega, N. J. Millam, M. Klene, J. E. Knox, J. B. Cross, V. Bakken, C. Adamo, J. Jaramillo, R. Gomperts, R. E. Stratmann, O. Yazyev, A. J. Austin, R. Cammi, C. Pomelli, J. W. Ochterski, R. L. Martin, K. Morokuma, V. G. Zakrzewski, G. A. Voth, P. Salvador, J. J. Dannenberg, S. Dapprich, A. D. Daniels, Ö. Farkas, J. B. Foresman, J. V. Ortiz, J. Cioslowski and D. J. Fox, Gaussian, Inc., Wallingford CT, 2009.
- [5] *Gaussian 16, Revision C.01*, M. J. Frisch, G. W. Trucks, H. B. Schlegel, G. E. Scuseria, M. A. Robb, J. R. Cheeseman, G. Scalmani, V. Barone, G. A. Petersson, H. Nakatsuji, X. Li, M. Caricato, A. V. Marenich, J. Bloino, B. G. Janesko, R. Gomperts, B. Mennucci, H. P. Hratchian, J. V. Ortiz, A. F. Izmaylov, J. L. Sonnenberg, D. Williams-Young, F. Ding, F. Lipparini, F. Egidi, J. Goings, B. Peng, A. Petrone, T. Henderson, D. Ranasinghe, V. G. Zakrzewski, J. Gao, N. Rega, G. Zheng, W. Liang, M. Hada, M. Ehara, K. Toyota, R. Fukuda, J. Hasegawa, M. Ishida, T. Nakajima, Y. Honda, O. Kitao, H. Nakai, T. Vreven, K. Throssell, J. A. Montgomery, Jr., J. E. Peralta, F. Ogliaro, M. J. Bearpark, J. J. Heyd, E. N. Brothers, K. N. Kudin, V. N. Staroverov, T. A. Keith, R. Kobayashi, J. Normand, K. Raghavachari, A. P. Rendell, J. C. Burant, S. S. Iyengar, J. Tomasi, M. Cossi, J. M. Millam, M. Klene, C. Adamo, R. Cammi, J. W. Ochterski, R. L. Martin, K. Morokuma, O. Farkas, J. B. Foresman, and D. J. Fox, Gaussian, Inc., Wallingford CT, 2016.